



Queensland University of Technology
Brisbane Australia

This may be the author's version of a work that was submitted/accepted for publication in the following source:

Javanroodi, Kavan, [Nik, Vahid](#), & Mahdavinejad, Mohammadjavad (2019)

A novel design-based optimization framework for enhancing the energy efficiency of high-rise office buildings in urban areas.

Sustainable Cities and Society, 49, Article number: 101597 1-21.

This file was downloaded from: <https://eprints.qut.edu.au/129562/>

© Consult author(s) regarding copyright matters

This work is covered by copyright. Unless the document is being made available under a Creative Commons Licence, you must assume that re-use is limited to personal use and that permission from the copyright owner must be obtained for all other uses. If the document is available under a Creative Commons License (or other specified license) then refer to the Licence for details of permitted re-use. It is a condition of access that users recognise and abide by the legal requirements associated with these rights. If you believe that this work infringes copyright please provide details by email to qut.copyright@qut.edu.au

License: Creative Commons: Attribution-Noncommercial-No Derivative Works 4.0

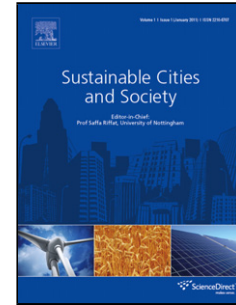
Notice: *Please note that this document may not be the Version of Record (i.e. published version) of the work. Author manuscript versions (as Submitted for peer review or as Accepted for publication after peer review) can be identified by an absence of publisher branding and/or typeset appearance. If there is any doubt, please refer to the published source.*

<https://doi.org/10.1016/j.scs.2019.101597>

Accepted Manuscript

Title: A novel design-based optimization framework for enhancing the energy efficiency of high-rise office buildings in urban areas

Authors: Kavan Javanroodi, Vahid M. Nik, Mohammadjavad Mahdavinejad



PII: S2210-6707(19)30406-8
DOI: <https://doi.org/10.1016/j.scs.2019.101597>
Article Number: 101597

Reference: SCS 101597

To appear in:

Received date: 10 February 2019
Revised date: 5 May 2019
Accepted date: 9 May 2019

Please cite this article as: Javanroodi K, Nik VM, Mahdavinejad M, A novel design-based optimization framework for enhancing the energy efficiency of high-rise office buildings in urban areas, *Sustainable Cities and Society* (2019), <https://doi.org/10.1016/j.scs.2019.101597>

This is a PDF file of an unedited manuscript that has been accepted for publication. As a service to our customers we are providing this early version of the manuscript. The manuscript will undergo copyediting, typesetting, and review of the resulting proof before it is published in its final form. Please note that during the production process errors may be discovered which could affect the content, and all legal disclaimers that apply to the journal pertain.

A novel design-based optimization framework for enhancing the energy efficiency of high-rise office buildings in urban areas

Kavan Javanroodi^{a,d}, Vahid M. Nik^{a,b,c}, Mohammadjavad Mahdavinejad^d*

^a *Division of Building Physics, Department of Building and Environmental Technology, Lund University, SE- 223 63, Lund, Sweden (kavan.javanroodi@byggttek.lth.se, vahid.nik@byggttek.lth.se, nik.vahid.m@gmail.com)*

^b *Division of Building Technology, Department of Civil and Environmental Engineering, Chalmers University of Technology, Gothenburg, Sweden (vahid.nik@chalmers.se)*

^c *Institute for Future Environments, Queensland University of Technology, Garden Point Campus, 2 George Street, Brisbane, QLD, 4000, Australia (vahid.nik@qut.edu.au)*

^d *Department of Architecture, Art and Architecture Faculty, Tarbiat Modares University, Tehran, Iran (kavan.javanroodi@modares.ac.ir; Mahdavinejad@modares.ac.ir)*

* *Corresponding Author*

Highlights

- A multi-objective optimization framework to find optimal forms in urban areas
- With a novel design-based approach emphasizing on geometry and energy calculations
- 1998 optimal form combinations generated and studied considering urban microclimate
- 34% energy demand and 12% thermal discomfort reduction adopting the framework
- A series of design-based recommendations presented for early-design stage

Abstract

Designing high-rise buildings is a complex and challenging task involving several parameters and variables. Recently, there have been major attempts to design the overall form of these buildings based on optimization approaches. This paper introduces a multi-objective optimization framework based on Genetic Algorithm, namely Energy Efficient Form-finder (EEF), consisting four main steps of Form-Generation, Form-Simulation, Form-Optimization and Form-Solutions. The EEF with a comprehensive design-based approach is evaluated through five functions considering objectives of minimizing cooling and heating demand and thermal discomfort time while maintaining operative temperature on the defined thermal comfort zone.

This work studies the form combination of five reference buildings based on a new technique called “Building Modular Cell” in five different urban areas, resulting in twenty-five distinct design problems. According to the results, there is a great potential to adopt EEF in newly-built projects with a rectangular layout; while it can reduce the annual energy demand and thermal discomfort time of the optimal form combinations around 34% and 12% respectively. Finally, a series of qualitative and quantitative design-aid recommendations are presented based on 1998 best design solutions, which can be used as form-finding rules of thumb by architects and urban designers at the early design stages.

Keywords: design-based framework; multi-objective optimization; early design stage; energy demand; thermal discomfort time; urban microclimate;

Nomenclature			
A_{surf}	Area of external surface [m ²]	SC	Site coverage
A_f	Area of front elevation [m ²]	S_i	Sensitivity Index
ANN	Artificial Neural Network	T_{db}	Dry-bulb temperature [°C]
A_p	Plot area of surrounding buildings [m ²]	T_{rt}	Mean radiant temperature [°C]
A_s	Site area in a horizontal section [m ²]	T_m	Monthly average temperature [°C]
A_t	Total area of all floors [m ²]	T_n	Neutrality temperature [°C]
A_i	Total area of generated form in floor I [m ²]	T_o	Operative Temperature [°C]
BMC	Building Modular Cells	T_{os}	Operative Temperature in summer [°C]
BD	Building Density	T_{ow}	Operative Temperature in winter
EEF	Energy Efficient Form-finder	T_{owin}	Operative temperature in winter function
GH	Grasshopper	TDT	Thermal Discomfort Time function
GA	Genetic Algorithm	VAR	Volume area ratio
MS_i	Comfort time in summer [h]	V	Final volume of combination [m ³]
MW_i	Comfort time in winter [h]	V_{BS}	Mean value of best solutions
PAR	Plot Area Ratio	V_{WS}	Mean value of the worst solutions
Q_C	Cooling energy [kWh]	UD	Urban Density
Q_H	Heating energy [kWh]	WWR	Window to wall ratio
q_H	Heating demand function [kWh/m ²]	λ_f	Frontal area density
q_C	Cooling demand function [kWh/m ²]	λ_p	Urban plan area density
Rc	Relative compactness	γ	Radiative fraction

1. Introduction

According to the UN, the global urban population will increase from 3.8 billion in 2014 to 7.6 billion in 2050; where megacities in developing countries with middle-income economy are responsible for a large portion of this growth [1,2]. Consequently, the share of urban areas in the world final energy consumption (70% in 2014) is expected to increase, especially due to the demand from building sector [3,4]. Studies have predicted that the portion of energy consumption for commercial buildings will increase notably while tend to decrease in residential buildings during the next two decades [5]. Heating and cooling are accounted for more than 48% share of the annual energy demand to achieve indoor thermal comfort in office buildings; a huge category which includes 23% of non-residential buildings globally [6,7]. Climate change may vary this share due to higher average air temperature and more frequent and stronger extreme conditions [8,9], inducing undesired variations in the average and peak cooling and heating demand as well

as thermal discomfort [10,11]. For instance, mean air temperature has increased up to 0.27°C in the United States during the last decade [12], while in Europe has been around 1.7°C above the pre-industrial level and is expected to exceed between 1 to 2°C by 2050 [13]. Supplying energy in a sustainable manner for urban environments is a topic of broad and current interest, where many studies point to the benefits and potentials of integrating renewable energy generation through decentralized energy systems and micro-grids [14,15]. The role of urban design and its effects on the microclimate conditions and the energy performance of buildings can be considerable and support the movement of societies towards climate change mitigation and adaptation as well as 100% renewable energy systems.

The consequences of urban growth and climate change may become more crucial in developing countries such as Iran with rapid urbanization (urban population from 25.9 million in 1987 to 59.4 million in 2016 and up to 78.4 million in 2050) [13] and high energy consumption rate (five times higher than the world average) [16]. For example, the average electricity consumption growth in Iran (7.9%) is more than twice of the global average (3.3%) [17]. Annual energy demand for office buildings in Iran is about 350 kWh/m^2 , which considering working hours (8 to 10 active hours per day), is notably higher than the world's average [18]. Heating and cooling are accounted for 55% of total annual energy consumption of office buildings in Iran [19]. The minimum air temperature in Iran has increased up to 0.34°C in a forty-year period (from 1961-2010) and is expected to increase at a higher rate in the following decades [20]. Several other factors are worsening the conditions such as inefficient building designs and constructions as well as the lack of effective building codes and regulations for having low-energy and sustainable buildings. Although some progress have been made (the most recent one is National Construction Regulation No.19 [21]), results are not satisfying at the practical level.

There have been major attempts worldwide to establish practical efficient building codes such as LEED in the US, CGBL in China, DGNB in Germany, Miljöbyggnad and FEBY in Sweden [22], HQE in France and BREEAM in UK [23,24]. However, as one might expect, a new trend of optimized building regulations and codes for office buildings is required to face the complexities of the growing energy and climate concerns, rather than confining to current building codes and typical design approaches. Designing office buildings with respect to urban microclimate, conceptual values of architects and future energy challenges at the same time, is a demanding task and needs to take several parameters and constraints into account.

In the design firms, architects and urban designers are the key decision makers in the design process. But, they usually tend to use invalidated passive design methods based on “trial-and-error”. Lately, optimization approaches have been applied by researchers during design process of buildings and urban areas, combined with building energy simulations [25]. A common approach in building design process is “simulation-based optimization”, combining numerical simulations and optimization algorithms [26,27]. In design problems, always more than one objective is engaged with the process; this pushes the assessment towards multi-objective optimization and considering all the influencing parameters and constraints. Accordingly, several simulation-based optimization algorithms have been developed for multi-objective problems such as evolutionary algorithm (including genetic algorithm, Particle Swarm optimization [28,29], Ant Colony

Optimization [30,31]), derivative-free search methods and hybrid algorithms or other Meta-heuristic models like Artificial Neural Network combined with NSGA-II [32,33]. Three main streams can be recognized in the available studies and platforms for multi-objective optimization in building and energy studies, including (a) using generic programming platforms for linear or non-linear optimization problems such as: *Matlab* [34–36], *GenOpt* [37,38], *CAMOS* [39,40] and modeFRONTIER [41,42]; (b) combining tools for coupling BIM tools, EnergyPlus, TRANSYS, DOE-2 as simulation stage with generic programming platforms for optimization phase [43–45]; (c) adopting graphical interfaces for modeling (e.g. Grasshopper in *Rhinoceros* and Dynamo in Autodesk Revit), simulation (e.g. Diva/Archsim, RADIANCE, Honeybee and Ladybug, etc.) and optimization (e.g. GA based plugins like *Galapagos*, *Octopus*, *Optimo*, etc.) [46–48].

By means of these platforms and tools, numerous research works focused on optimizing parameters such as building envelope geometry [49,50] or materials [51,52], insulations [53,54], openings and glazing [55,56], shading [57,58] for one or several reference case studies in terms of energy efficiency and consumption (heating, cooling and lighting) [7,59,60], thermal comfort [61–63], visual comfort [64–66], air temperature [67–69], ventilation and HVAC [70–72] as objectives at different stages of the design process. However, these studies have focused on some certain parameters and have not addressed the whole design process of a building; and their results are still complicated and ambiguous for design teams which are usually led by architects and urban designers. Thus, there have been some attempts to assign multi-objective optimization approaches into the design process of buildings for designers. Zhang et al [73], adopted three typical school layouts in China with different orientation, WWR, glazing, shading and corridor depth to find optimal trade-off between heating and lighting energy, summer discomfort time and useful daylight illuminance. Negendahl and Nielsen [74] introduced a method to optimize building variables in terms of energy consumption and solar radiation at the early design stages which confined to three set of main building layout variations. Yu et al. [75] used genetic algorithm for optimization of several variables of one residential building to maximize energy efficiency and indoor comfort. Wright et al [76] used genetic algorithm to optimize thermal comfort against energy cost of a sample building and HVAC system. Most of these studies have used predefined case studies with some unique solutions, only applicable for the introduced condition and design-problem, or have developed analytical forecasting frameworks to predict and evaluate building performances which are not based on real constraints and not applicable in practice for designers [77–79]. Moreover, a comprehensive optimization framework with a back and forth loop to consider all influencing parameters, objectives and constraints in the form-finding procedure is still missing in the available literature.

To address this research gap, the current study introduces a novel design-based optimization framework for reducing the annual energy demand (i.e. cooling and heating) and thermal discomfort in high-rise office buildings while maintaining the operative temperature. The framework emphasizes on the geometry, form and architectural aspects of the building/urban design as well as detailed energy demand calculations. The introduced framework has the ultimate aim of developing an easy-setup framework for newly-built design projects enabling to follow an energy efficient form-finding process at the early design stage. Moreover, the acquired databases of the results have the potential of being implemented in newly built high-rise buildings by bridging the gap between designers and engineers. For the purpose of this work, a twelve-story

office building was taken as the reference case in Tehran, the capital city of Iran with high urban population, various urban densities and multiple long lasting hot and cold months [80,81]. Considering the big challenge of reducing energy consumption while attaining the thermal comfort in office buildings (which are occupied at least one-third of a day [82]), five objective functions are defined in this study. These functions are designed to minimize the cooling demand, heating demand and thermal discomfort time as well as maintaining the operative temperature in the defined comfort zone during both hot and cold seasons. The impacts of urban morphology on the energy demand and thermal comfort calculations is also considered by defining five detailed urban models for each optimization problem. This results in twenty-five independent optimization problems.

The article is structured as follows: in the methodology section, the theoretical background, novel approach and proposed framework are discussed extensively. Moreover, the simulation tools, inputs, weather data and workflow are presented in four main steps including Form-generation, Form- simulation, Form-optimization and Form-solutions. In the results and discussion section, the major findings of the defined optimization problems are presented for each considered urban area and high-rise building typology. Accordingly, a series of qualitative and quantitative design-based recommendations are derived out of the acquired database. Finally, a summary of the main findings as well as the probable applications of the introduced framework are discussed in the conclusion section.

2. Methodology

2.1 The theoretical background

Optimization can be defined as the process of finding the best solutions through minimizing or maximizing certain objectives considering certain constraints [83]. The performance and selection of an optimization algorithm mainly depends on the nature and scale of the problem. Several studies indicate that using genetic algorithm (GA) is very efficient, fast and accurate approach for the whole building simulation [84–86]. There are several methods to find the best answers out of a multi-objective optimization problem using GA [87]. Among them, Pareto-dominance approach is generally accepted as the best way to optimize all objectives simultaneously [23]. It also provides a set of non-dominated solutions which can be selected and used by designers. The applicability of the provided solutions in practice depends on the defined constraints and objectives. Research works with some predefined design constraints have a lower process-time due to limiting the search space; while the flexible geometric constraints result in more realistic solutions that take longer process time [74]. Thus, the optimization problem should be defined in an efficient way to consider flexible design-based parameters and variables as well as other architectural values.

By using visual programming languages (VPL) and coupling a series of tools in a framework, higher flexibility will be provided for designers to study a higher number of design-solutions while maintaining the qualitative aspects of their design and concept [88]. Some research works have attempted to develop such a framework based on the widely-available tools in the architectural research and design firms [89,90]. Konis et al. [91] developed a framework to improve the performance of daylighting, solar control and natural ventilation potential strategies of a site-specific building according to simulation-base GA optimization approach. Aiming at maximizing solar gains, Zhang et al [92] proposed a modeling-simulation-optimization framework for designing free-form buildings based on two physical parameters: space efficiency and shape

coefficient as the geometric constraints to optimize solar radiation gain. Yi and Malkawi [93] presented an optimization process for building form based on geometry control points (flexible geometric constraints) to achieve optimal heat gain and heat loss. Several other studies have introduced optimization frameworks for buildings and urban models focusing on solar irradiation [94,95] and heat gain [96,97]. The outcomes of these optimization frameworks are mostly limited to non-geometrical variables, very complex multi-facades, non-constructible shapes or have confined only to few cases and/or small buildings that cannot cover the form-finding process for the designers. In this study, through adopting VPL, a series of modeling, simulation and optimization tools are coupled with the aids of several flexible constraints and objective functions. Instead of focusing on one element of a building or an architectural space, the overall form of the building is optimized by introducing a comprehensive framework. Several parameters and design variables are taken into account in this framework including the layout geometry, final height, material, glazing and orientation in a multi-objective optimization algorithm.

2.2 Multi-objective Framework

The proposed multi-objective optimization framework, namely “Energy Efficient Form-finder” (EEF), is a replicable framework based on a developed version of “Building Modular Cells” (BMC) for the form-finding process of high-rise office buildings in urban areas. In an earlier work of the authors [98], BMC technique was introduced and validated to evaluate the impacts of urban morphology on cooling demand and ventilation potential. The developed version of BMC technique is used in this study for initial form generation as the first step, a script that enables generating thousands form combinations in five urban areas (check Section 2.2.2). The EEF optimization framework consists of four main comprehensive steps including (1) Form-generation, (2) Form-Simulation, (3) Form-Optimization and (4) Form-Solutions; where each step includes several integrated phases (Figure 1). At Step (1), the urban morphology and BMC technique is defined according to design problem characteristics and parameters such as building material, glazing and orientation. The form combinations can be generated based on an innovative GH algorithm; in which, BMC technique [98] was developed in detail for a cuboid building in the context of five selected urban morphologies of Tehran (Section 2.2). The developed version is used for initial Form-generation step with 30826 possible form configurations in each urban area; resulting in 154130 unique possible form combinations (based on the mathematical combinations of the forms in the defined grids in the layout). Moreover, several sensitivity analyses were conducted for finding the most important influencing design-based parameters and constraints to be considered in the optimization process for the reference building.

In Step (2), the urban microclimate and weather data of selected urban areas are assigned to the generated form combinations and applied to simulation engines for cooling and heating demand, thermal discomfort and operative temperature during both cold and warm seasons. The thermal comfort calculations are carried out based on the defined comfort zone according to ASHRAE 55. Furthermore, a validation study is conducted as a key factor for verifying the accuracy of the thermal discomfort time (TDT) calculations. At Step (3), objective functions, their constraints and optimization problems are adjusted according to the design problem, aiming at extracting the best design solutions out of Pareto-front graphs. Multi-objective optimization platforms for twenty-five independent optimization problems were run to include all possible conditions into the framework

and provide a database for design-based suggestions. At the final step, form-solutions which can be adopted in different design problems are extracted and analyzed. Moreover, the design-based suggestions are derived out of top optimal form combinations in each urban area (1998 best design solutions). Figure 1 shows the schematic flowchart of the proposed framework.

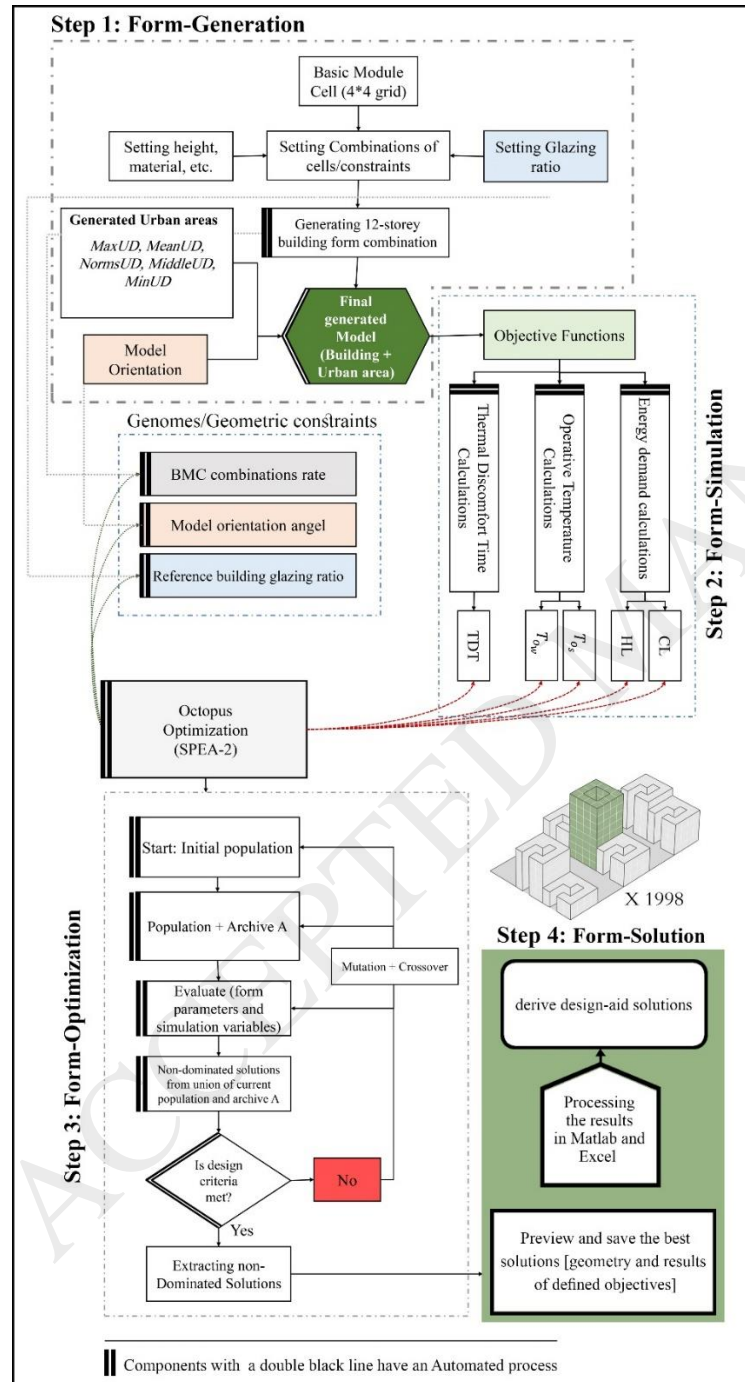


Figure 1, The schematic flowchart of Energy Efficient Form-generation (EEF) framework (Components with a Blue line have an Automated process) for one optimization problem with a distinct BMC range (the flowchart for generating five urban areas is excluded from the flowchart).

2.3 Step (1): Form Generation

2.3.1 *The urban area*

It is commonly accepted that urban morphology has a major impact on building performance [99] and its role should be considered in building simulation procedure [100]. Thus, as the case study, urban morphology and microclimate of Tehran was considered in the building performance simulation process. Tehran is located at the latitude and longitude of 35.69°N and 51.42°E [101] with a semi-arid climate [102], having cold winters (e.g. minimum of -10°C in January), hot-arid summers (e.g. maximum of 40°C in July) [103], the annual relative humidity of 41% and rainfall of 233 mm [80]. The city has experienced a rapid urbanization during last six decades (from 1.8 million populations and 100 km² total land coverage in 1956 to 8.37 million and 730 km² in 2016) [81]. Tehran has evolved to a megacity with twenty-two municipal districts, each with a strong tendency to accommodate high-rise office buildings. Thus, a high-rise building selected as the reference building in this study and the urban area was modeled based on the typical surrounding buildings around high-rise buildings in Tehran.

The physical characteristics of urban neighbourhoods in twenty-two municipal districts of Tehran were recognized and categorized (See Figure A.1 in Appendix for a summary of the findings). A hypothetical site with nine equal square blocks (a matrix with three rows and columns where one of the blocks at the center of the site considered as the main high-rise building site) was defined as the main urban platform and 1600 urban configurations were modelled based on three introduced parameters (urban pattern, urban building form and urban density). The most comprehensive parameter which was used for generating the layouts, plans and heights of buildings in these urban platforms was urban density (UD) with five ranges from Min (35.8% site coverage and thirty total number of floors*) to Max (85.6% site coverage and fifty-two total number of floors). The height of the surrounding buildings were considered from two-story up to twelve-story (two/four-story as low-rise, six/eight-story as mid-rise and ten/twelve-story as high-rise buildings) according to each UD (the reader is referred to [98] for more details). To consider the impacts of urban morphology and microclimate on the proposed framework, five urban areas based on the UD ranges with distinct urban building forms were selected out of the best urban configurations, representing the urban areas in Tehran. Figure 2 shows the selected urban areas based on some of the considered indicators such as VAR, SC, PAR and BD, which is used to define UD. Using these five selected urban areas, the BMC technique was developed for designing and optimizing the form of central high-rise urban block.

2.3.2 *Developed BMC technique and the reference building*

The BMC technique is based on an 8×8 m rectangular module; these dimensions are selected according to the typical reinforced concrete structures in Tehran, in which the height of each floor is 4m. This modular grid can be assigned to a large part of typical office buildings in Tehran, according to existing building codes, regulations and the mentioned survey study [98]. Based on a sensitivity analysis and considering “speed” and “accuracy” as the key factors of a replicable framework, 4×4 grid cells for each sub-site selected as the main modeling platform for the form-generation step (Figure 3). By using this grid resolution with 30826 possible form combinations, almost all the well-known building forms (L, U, CY, C, T etc.) and hundreds of new combinations

* The total number of floors of surrounding buildings in one urban case study with certain distributions

can be covered with a 100 times faster runtime compared to higher grid resolutions (5×5 or 6×6). The other design variable constraints are defined based on series of form combination rules (this is discussed thoroughly in Section 2.3.3).

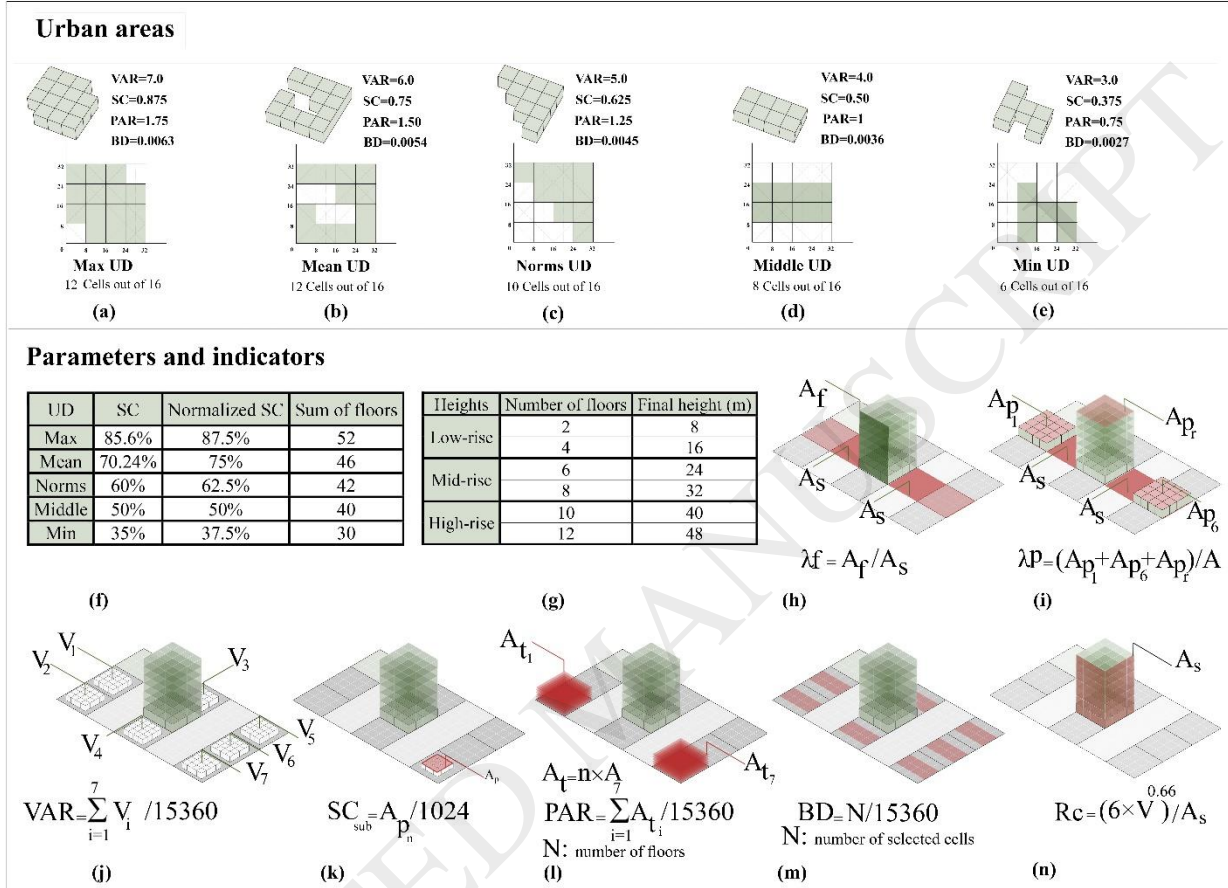


Figure 2. **Top:** Selected urban areas based on UD: (a) Urban area with MaxUD, (b) Urban area with MeanUD, (c) Urban area with NormsUD, (d) Urban area with MiddleUD, (e) Urban area with MinUD.

Bottom: urban morphology parameters and indicators used in this study to define urban density: (f) the five ranges of UD: site coverage and total sum of the floors, (g) six types of building's height defined in this study, (h) urban plan area density (λ_p): the built area projected onto the ground surface divided by the site area in a horizontal section (A_s), (i) frontal area density (λ_f): is the area of frontal surface of façade to the A_s , (j) volume area ratio (VAR): total volume of surrounding buildings divided by the total site area of site (24000 m²), (k) site coverage (SC) the total area of the ground floor of the building divided by 1600 (the area of each sub-site: 40×40m), (l) plot area ratio (PAR): total floor area of the surrounding buildings divided by the total site area, (m) building density (BD): number of selected cells divided by the total site area, (n) Relative compactness (Rc): V: final volume of combination, A_s area of external surface.

(The process of generating these five urban areas is thoroughly described and validated in a previous work of authors[98].)

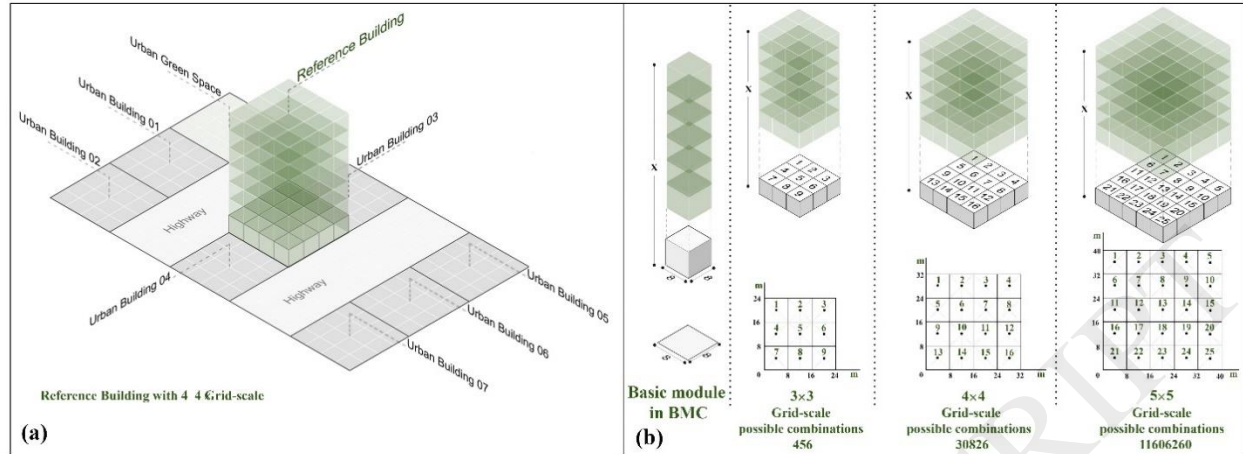


Figure 3. (a): The hypothetical site with a sample twelve-story reference building based on 4×4 grid.
 (b): the BMC module and its layouts for three different grid scales (3×3 , 4×4 and 5×5)

2.3.3 Form combination rules

As stated, five urban density ranges were normalized to a site coverage indicator of the central urban block according to the basic BMC module, resulting in five BMC ranges:

- 1) Max BMC: 87.5%, selecting 14 cells out of 16.
- 2) Mean BMC: 75%, selecting 12 cells out of 16.
- 3) Norms BMC: 60%, selecting 10 cells out of 16.
- 4) Middle BMC: 50%, selecting 8 cells out of 16.
- 5) Min BMC: 35.8%, selecting 6 cells out of 16.

According to these ranges, in each UD, five form configuration platforms from Max to Min BMC can be generated (twenty-five distinct situations), which can result in 154310 possible form combinations (based on mathematical combinations to select five BMC ranges out of sixteen cell-grid). Since the form-finding process of this study is based on discrete BMC ranges (defined as fixed integers in the algorithm), a series of geometric constraint on the design variables are required to limit the number of unnecessary iterations. a large part of the possible combinations can be excluded from the process due to their non-logical forms and non-significant differences in their thermal loads. Thus, a series of flexible geometric constraints were introduced as “form combination rules” in the modeling-optimization process. Figure 4 shows two basic design variable constraints s: 1) selected cells must be connected from their sides and not through their corners (based on structural and architectural logics: as each module can be considered as a simple room, there should be a connection from one of their sides to placing at least an entrance door), and 2) in all selections, only one integrated form must be chosen (configurations with two separate forms are not allowed); showing some true and false form combinations based on UDs.

Analysis showed that the most frequent false form combinations are non-integrated (unified) forms. The parametric process of generating cases is adjusted automatically using an innovative GH algorithm with the aid of Python script to handle the constraints. Thus, several built-in components and functions in GH are developed in the defined algorithm. Through this algorithm, eligible cases which have satisfied all the imposed constraints are selected out of the form-finding

process before getting to the simulation step. This results in lower process time while maintain the highest possible accuracy of search domain. According to the official building codes of Iran, a high-rise structure is a building with twelve or higher floors [104–106]. Thus, in this paper, each generated layout of the reference building based on the introduced form combination rules is extruded to 48m or twelve floors in the GH algorithm. The final height of the reference building in EEF framework can be varied based on the requirement of each design project.

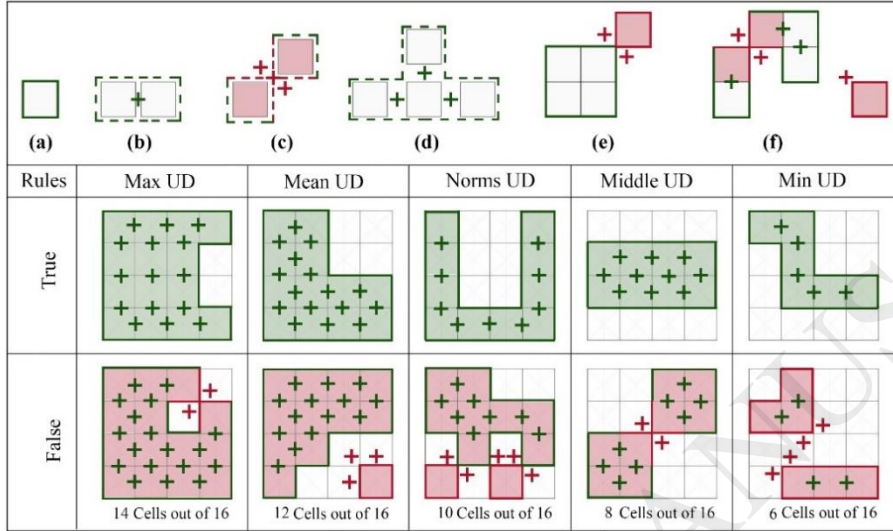


Figure 4. **Top:** Form combination rules as geometric constraints: (a): the 8×8 module cell, (b) and (d): selected cells must be connected from their sides, (c): connection from edges are not acceptable, (e): unacceptable cell connection from edges, (f) detached selected cell and edge connection. **Bottom:** some examples of True and False of form combinations based on the introduced form combination rules

2.3.4 Influencing parameters and sensitivity analysis

In addition to the main parameters considered in BMC technique, there are several other parameters that affect the energy performance of buildings due to the inherent uncertainties of the input data. By running hundreds of simulations and considering the influencing parameters, six parameters (glazing, shading, orientation, insulation, internal thermal mass and glass type) were selected, analyzed and ranked by their impact on the five objectives of the study (See Table B.1 in Appendix B), using a sensitivity index:

$$SI = \frac{V_{WS} - V_{BS}}{V_{WS}} \times 100\% \quad Eq (1)$$

The objectives of the study were sensitive to the variations of orientation and glazing ratio. Although insulation has a high sensitivity index, it is usually selected by engineers and not architects or urban designers, thus it was not considered as a main genome for the optimization function. Parameters such as shading and internal thermal mass induced a lower cooling and heating demand and TDT during summer and winter, while their impact on the simulation results was not considerable. Thus, in addition to the five ranges of the BMC, a several orientation angles are considered as genome (0, 15, 30, 45, 60, 75 and 90 degree). Furthermore, six glazing ratios (16%, 25%, 36%, 42%, 49% and 64%) are also assigned to the GA solver as genome. Other influencing parameters adjusted to the optimal value based on existing building codes and

regulations (Check Table B.1 in Appendix B for more detail about sensitivity index results). To limit the data uncertainties in the simulation stage, other uncertain variables such as user behavior and infiltration were also assumed as constant values due to comparative purposes of the study (See Table B.2 in Appendix B). The other data with possible uncertainties such as weather data or geometric constraints can be manually adjusted by the users in real applications. Moreover, due to comparative approach of the study, similar settings are applied to the modeling, simulation and optimization stages of each problem to minimize the impacts of data uncertainty on the results.

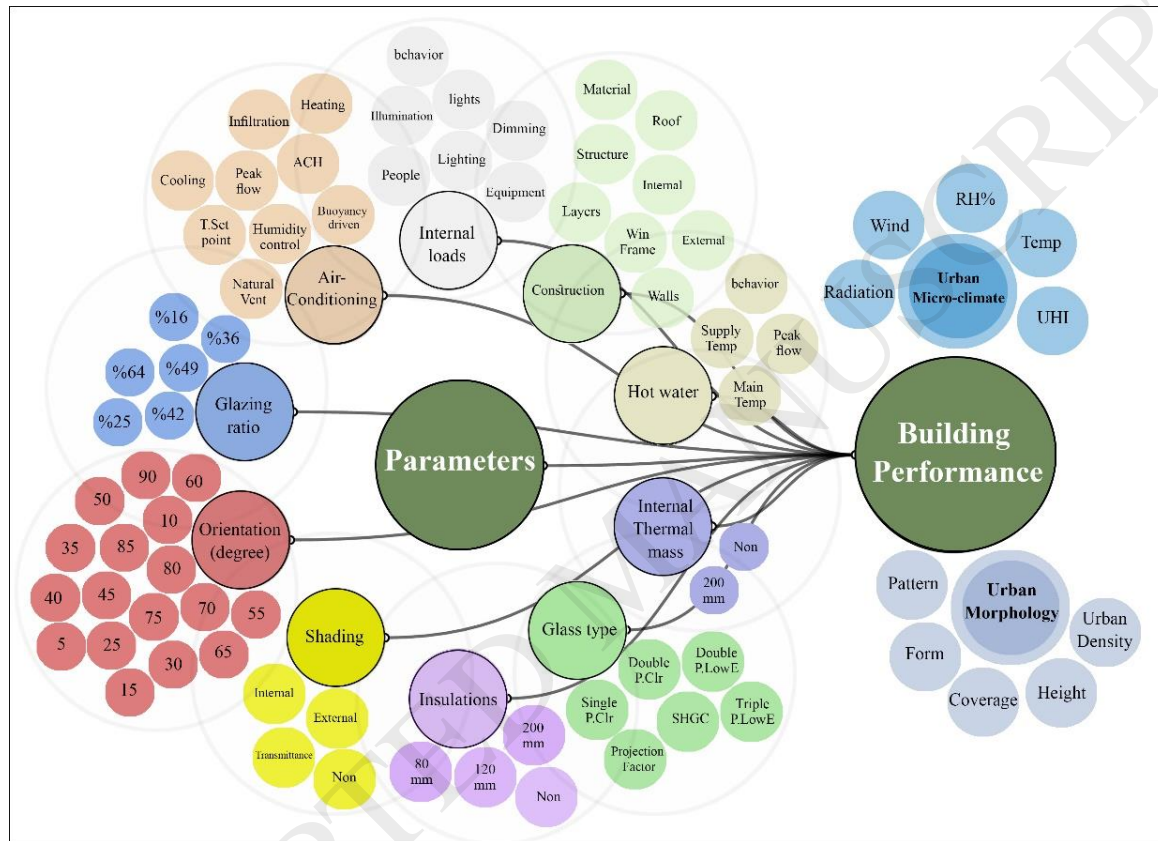


Figure 5. The influencing parameters with their assigned values in the simulation process

2.4 Step (2): Form-Simulation

2.4.1 Tools, inputs and weather data

Several design-based tools which are familiar for designers such as Rhinoceros/Grasshopper plugins (Diva-for-Rhino-Archsim, Ladybug tools and Octopus) and EnergyPlus are adopted in this study. At the first phase BMC technique was defined, modeled and prepared for simulations by the aid of an innovative GH algorithm. The geometry of eligible combinations out of the defined constraints are converted and exported into EnergyPlus by means of Archsim in the GH algorithm for energy simulations. The simulations are conducted according to the adjusted influencing parameters which were discussed in the former sections (Table B.1 and B.2 in Appendix B). At the final phase, a modeling-simulation-optimization loop is defined in the GH algorithm to ensure a back-and-forth process. In this process, hundreds of geometries are generated and simulated to optimize the final form of the reference building. The weather data of Tehran (based on EPW file

for Mehrabad Airport) with the hourly temporal resolution are used for simulating the hourly cooling and heating demand, TDT, T_{o_s} and $T_{o_{win}}$. The adopted weather data was validated for the urban microclimate of Tehran in the earlier work of the authors [98].

2.4.2 Objective functions

2.4.2.1 Cooling and Heating demand

The annual cooling and heating demand were defined as the sum of the latent and sensible cooling and heating energy. Each generated form combination is consisting of twelve floors and each floor has two zones: private office rooms and shared spaces. The calculated cooling and heating demand is affected by the heat transfer through building external surfaces (walls, roof, floors, windows, ceilings etc.) – known as building envelope – as well as the internal heat sources (people, appliances, equipment, lighting etc.) and infiltration through the building envelope and openings [108]. The annual cooling and heating energy demand are set for Tehran weather conditions; summer from April 1th to September 30th; winter from January 1th to March 31th and October 1th to December 31th. A number of inputs and other energy demand sources such as lighting, office equipment, hot water, infiltrations, residents etc. assigned to the models based on optimal values in national codes and regulations according to sensitivity analysis. To evaluate the impacts of building form on both cooling and heating demand and derive design-based suggestions considering all the influencing parameters, two objective functions were defined separately for energy demand in [kWh/m²].

$$q_C = \frac{\sum_{i=1}^n Q_{Ci}}{\sum_{i=1}^n A_i} \quad Eq (2)$$

$$q_H = \frac{\sum_{i=1}^n Q_{Hi}}{\sum_{i=1}^n A_i} \quad Eq (3)$$

Here, Q_{Ci} and Q_{Hi} are cooling demand and heating demand of each floor respectively. They are simulated using EnergyPlus engine. Two main constraints were imposed on the performance of the scheduled ventilation system during working hours to control operative temperature (the setting of the system is defined based on National Construction Regulation No.19 [21]). The maximum load limit of 100 w/m² with temperature set point boundary of 18 in winter and 27 in summer were considered in the calculations. The other parameters and constraints used in the simulations are presented in Table B.2 in Appendix. In the GH algorithm, cases with the minimize cooling and heating demand are selected as the best design solutions while maintain thermal comfort and operative temperature via minimizing the other defined functions.

2.4.2.2 Operative Temperature (T_o)

The operative temperature is defined according to ASHRAE 1995 which is the temperature of a uniform isothermal black enclosure in which the occupant exchanges the same amount of heat by radiation and convection as in the actual non-uniform environment [107]; or perceived environment temperature by the occupants considering convection and radiations. However, later ASHRAE proposed another method for calculating operative temperature considering air velocity rate for a better indication of the local thermal comfort which is used in this study. Here a weighted

mixture of radiant and air temperatures considering hourly air velocity range was used for calculating T_o by using “Object Zone control” in EnergyPlus:

$$T_o = \gamma T_{rt} + (1 - \gamma) T_{db} \quad Eq (4)$$

Here γ is radiative fraction – a non-dimension value – which is based on air velocity range [m/s] (from 0.3 to 0.9 according to hourly air velocity range from considered HVAC system and ACH in each generated case). In this work, T_o [$^{\circ}$ C] was calculated in each zone and the mean T_o [$^{\circ}$ C] for each floor was extracted and applied in Eq. (5) as objective function:

$$T_{o_s} = \sum_{i=1}^n \frac{T_{os_i}}{n} \quad Eq (5)$$

$$T_{o_w} = \sum_{i=1}^n \frac{T_{ow_i}}{n} \quad Eq (6)$$

T_{o_s} and T_{o_w} are the mean operative temperature in each floor for each generated case based on Eq (4) in summer and winter respectively. Where “n” is the number of floors which is twelve in this study. The operative temperature of the optimized solutions should not exceed the defined thermal comfort zone (Figure 12) as constraint. Thus, by defining a built-in component in the GH algorithm; the operative temperature in summer and winter were set to $T_{o_s} \leq 27$ and $18 \leq T_{o_w}$ to ensure the minimum and maximum boundaries of thermal comfort in the generated combinations with lowest energy demand. Due to the limitation of the applied GA algorithm; all defined objectives can only be minimized. Since, T_{o_w} should be maximized in the winter, another function was defined ($T_{o_{win}}$) and connected to the GH algorithm in Eq. (7):

$$T_{o_{win}} = (-1) \times T_{o_w} \quad Eq (7)$$

2.4.2.3 Thermal Discomfort Time (TDT)

Several methods have been introduced and applied in different research works for calculating and evaluating thermal comfort in the buildings; the most popular is Predicted Mean Vote (PMV) according to Fanger’s theory from ASHRAE 55 Adaptive model which is based on a correlation between indoor neutrality temperature and outdoor monthly mean temperature for air-conditioned buildings [23]. In this study, Thermal Discomfort Time (TDT) introduced as an easy-to-understand indicator which is the number of hours when the combination of humidity ratio and temperature is not in the comfort zone during summer (0.5 Clo.) and winter (1 Clo.). The comfort zone was defined according to the results of an extensive experimental and mathematical thermal comfort zone in Tehran by Heidari [108] based on McIntyre [109] and Humphreys [115,116] methods; where neutrality temperature T_n [$^{\circ}$ C] have the direct relation with T_m (monthly average temperature [$^{\circ}$ C]) in Eq (8):

$$T_n = 12.8 + 0.555T_m \quad Eq (8)$$

The psychometric chart and thermal comfort zone were generated using Ladybug tools (Figure 6) and its results were used for calculating temperature based on TMY weather file of Tehran and EnergyPlus engine in each floor and zone of the generated form combinations. The boundary of

relative humidity was defined from 38% to 66% according to thermal comfort measurements conducted by Heidari [110], as the humidity constraint. The optimization function for TDT is presented in a daily time step for easier comparisons as follow:

$$TDT = \sum_{i=1}^n \frac{MS_i}{N} + \sum_{i=1}^n \frac{MW_i}{N} \quad Eq (9)$$

In this equation, the number of points which are not in the boundary of defined constraints based on the comfort zone are summed up during summer and winter (MS and MW respectively) and divided by N which is equal to 24 [h]. In a parallel process, the calculations are verified using the operative temperature functions and their constraints for summer and winters using Archsim to ensure maintaining thermal comfort while the annual energy demand is minimized.

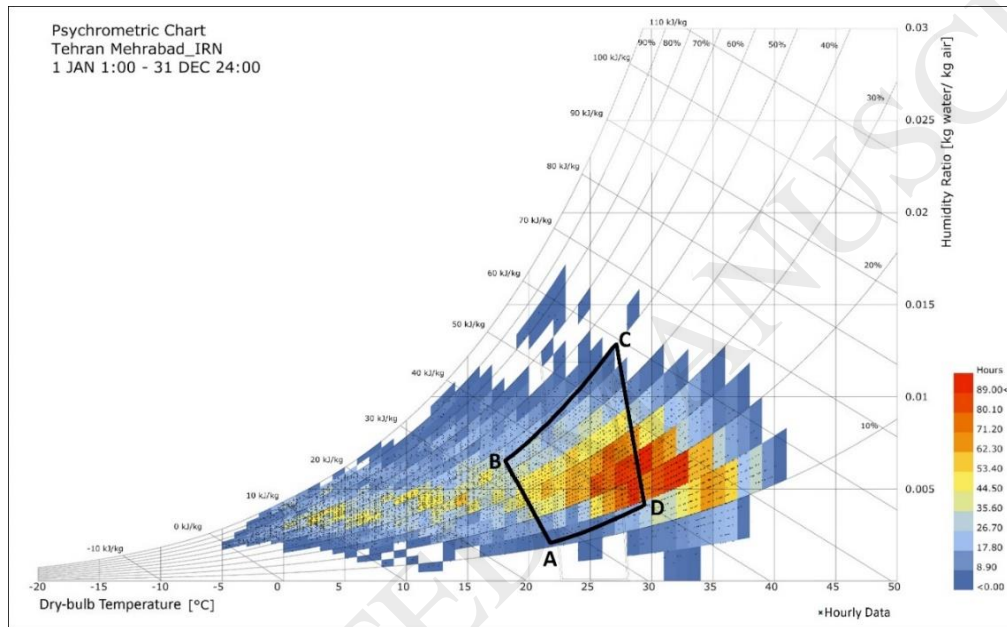


Figure 6. Psychrometric chart for Tehran, showing conditions for thermal comfort in summer and winter. The dots represent the number of hours inside and outside the comfort zone

2.4.3 Validation study of the simulation tools

A simplified cube sample room as one cell of BMC was constructed in real-scale to investigate the accuracy of adopted simulation tools for calculating thermal comfort (thermal discomfort time) and temperature. For this purpose, three 240×200×300 cm cuboid sample rooms were designed and constructed with polystyrene panels ($U=0.5 \text{ w/m}^2\text{K}$) and placed on the roof top of two adjacent four-story building with no obstacles at a distance of 15 meters from each side to avoid shading. Each sample room had a different doubled-glazed window (25%, 36% and 49% WWR ratio) at the south façade (check Table B.3 in Appendix B). A simple LSF (Lightweight Steel Frame) structure used for stabling the double polystyrene panels (240×100×10 cm each panel) as walls, floor and roof. Moreover, a combination of cored bricks with dry construction used at the floor of the sample room as thermal mass to control fast temperature fluctuations. A HOBO UX100_003 data logger installed in the center of the sample room at the H=110cm to avoid direct solar radiation from the window, and another data logger was placed outside the sample room to measure outside

temperature and relative humidity on an hourly time-step (an umbrella used to avoid direct solar radiation for the outside data logger). Summer and winter solstices (21 June and 21 January) selected to measure the most critical extreme temperature and thermal discomfort time in the all three sample rooms in 2016. On a parallel process, three sample rooms were modeled and simulated using the introduced framework (GH, Archsim, Ladybug, Energyplus) for the same date using EnergyPlus weather data to compare and verify the trends and the absolute results of both processes. Furthermore, the thermal discomfort time calculated based on measured temperature and relative humidity and calculated comfort zone in the psychometric chart (Figure 7) used for optimizing TDT in the study.

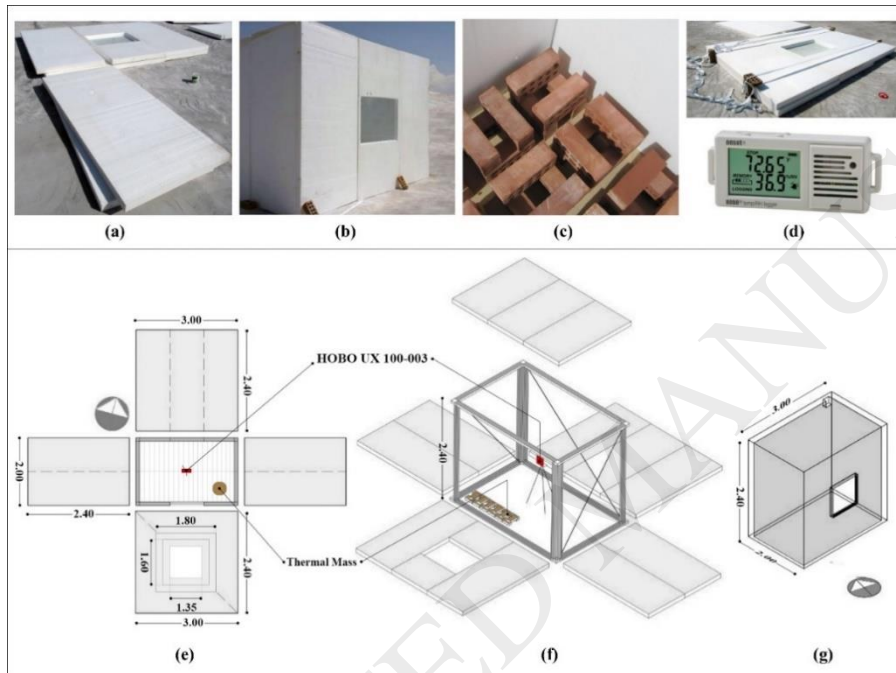


Figure 7. The characteristics of the sample room built for the validation study

Results showed that the variations of temperature were quite similar for both measured and simulated data; where sample room with higher WWR has a higher temperature and more TDT in both measured and simulated cases. The temperature difference between measured and simulated cases was from 4.7 °C for 25% WWR, 7 °C for 36% WWR and 10.61 °C for 49% WWR, and for 49% WWR and 25% WWR cases is 8.21 °C for measured data and 2.3 °C for simulated results (Figure 8). This notable temperature difference between measured and simulated results is due to higher UHI, greenhouse effect and heat flux in real case versus simulation model. The measured and simulated TDT (based on the defined thermal comfort zone in Figure 7) for the sample room with different WWR are shown in Table 1. According to the results, there is a good agreement between measured and simulated results, and TDT difference in all calculations is lower than 50 minutes. Thus, the adopted simulation tools to calculate TDT and temperature are accurate enough to be applied to the framework.

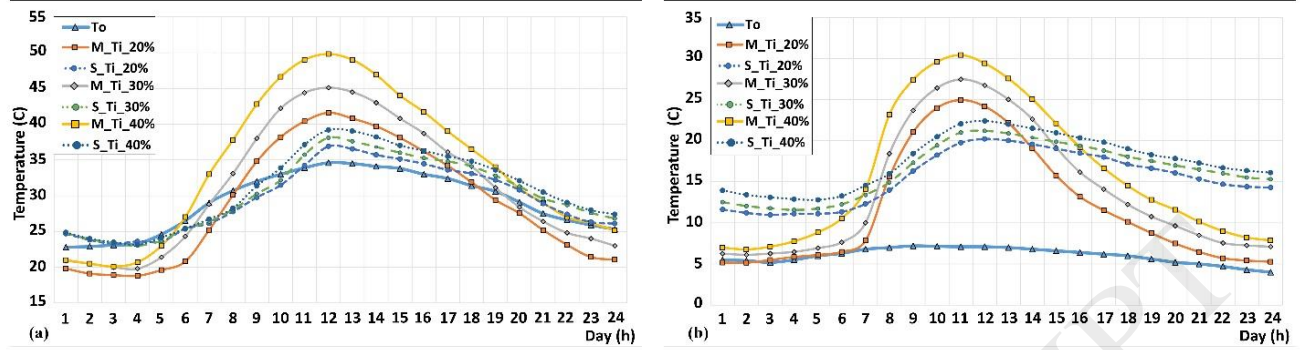


Figure 8. Hourly measured and simulated outdoor and indoor temperature for the sample room; (a) Summer 21 July, (b) Winter 21 January; T_i : Indoor temperature, T_o : Outdoor temperature, M : measured, S : simulated.

Table 1. Measured and simulated TDT for the sample room with different WWR

WWR	Season	Date	Hours	Measured TDT (h)	Simulated TDT	Differences
25%	Summer	21 July	24	15:25	14:46	00:39
	Winter	21 Jan	24	18:05	17:34	00:31
36%	Summer	21 July	24	15:56	14:08	00:12
	Winter	21 Jan	24	17:14	16:49	00:25
49%	Summer	21 July	24	16:21	15:43	00:38
	Winter	21 Jan	24	17:48	16:03	00:15

2.5 Step (3): Form-optimization

2.5.1 Defining optimization problems

The third step of the EEF framework, is the multi-objective optimization of possible form combinations. According to the survey on urban areas in Tehran [98], there is a correlation between the urban density of an area and the coverage of a newly-built building; the higher urban density, the higher site coverage. Thus, five distinct optimization problems can be defined based on five selected urban areas with the introduced UD. However, in order to consider all the possible conditions in the real design projects, the five defined ranges of BMC are considered in each urban area (five optimization problem in each UD). For instance, in MaxUD, five building optimization problems with Max, Mean, Norms, Middle and Min BMC (based on the site coverage) are defined. Optimization problems with similar UD and BMC are the main problems namely from 1 to 5 and the other problems are recognized from number 6 to 25 (Figure 9). In real applications only one UD can be selected by the design team as the main platform of the optimization study to reduce the optimization runtime and number of the unnecessary iterations. In the GH algorithm, five main loops (UDs) were connected to GA solver to explore the trade-offs between generated forms in each loop and the objectives to find best design solutions. Table B.4 in Appendix B shows the number of the non-dominated solutions found in each UD and BMC for all twenty-five optimization problems.

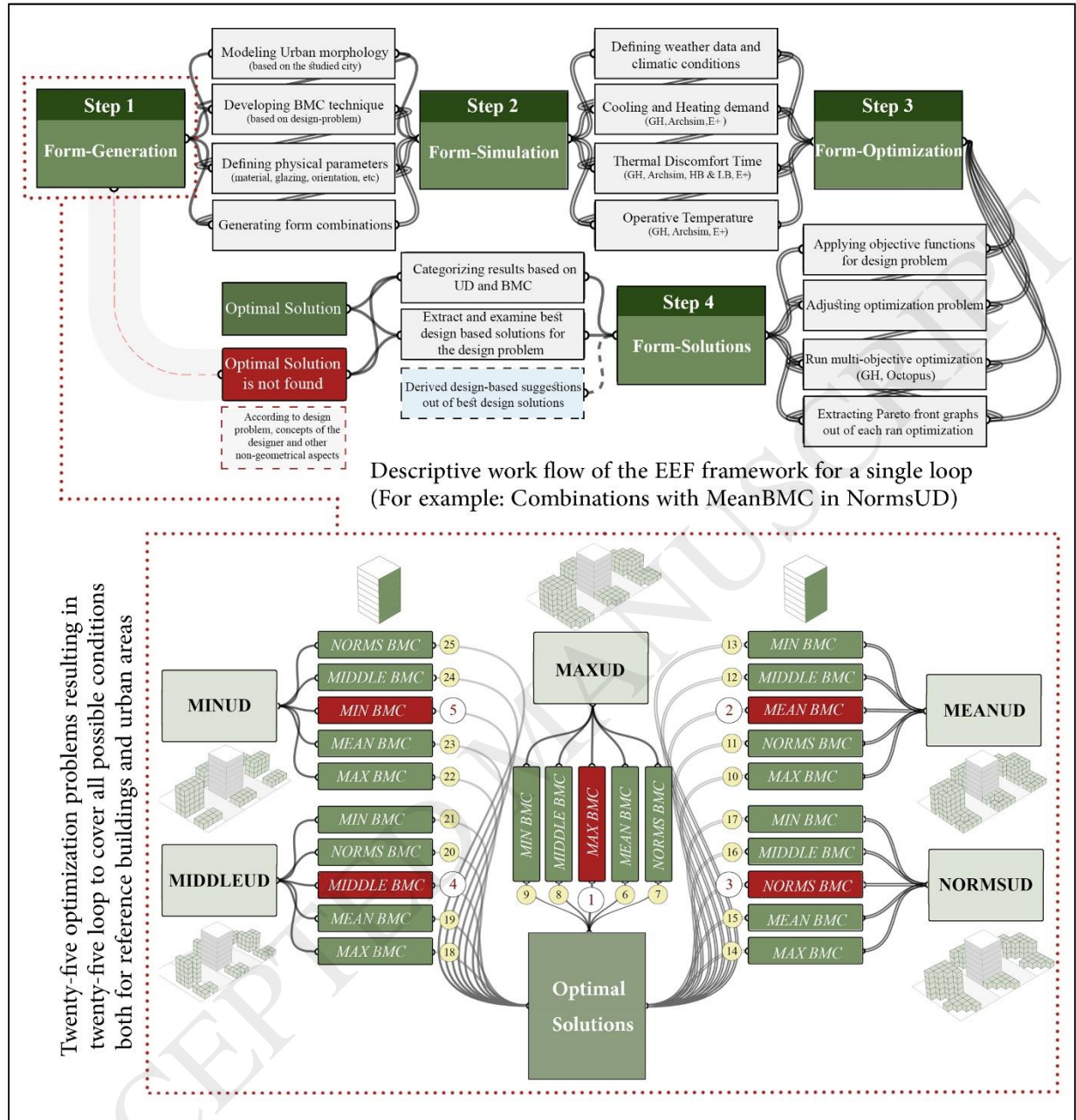


Figure 9. **Top:** Descriptive work flow of the EEF framework for a single loop

Bottom: Twenty-five defined optimization problems based on UDs and BMCs (the results of optimization problems 1 to 5 are discussed in more detail while the main findings of 6 to 25 are presented in brief for deriving design-based solutions).

The multi-objective optimization with 100 populations, maximum 40 generations, mutation rate of 0.5 and crossover rate of 0.8 with SPEA-2 reduction was performed for all twenty-five problems separately to get convergence through hundreds of iterations (average calculation time for each optimization problem was 7.6 h). The average runtime for each iteration for five introduced objectives was about 40s which is quite fast considering the calculation load; influencing parameters in the form generation; number of objectives; and the comprehensiveness of the study

for the early stage design. The optimizations are conducted using Octopus plugin (GA solver) in Grasshopper as discussed earlier. The main genomes connected to the Octopus component are BMC combination, orientation and glazing. For each optimization problem, a 3D-visual Pareto front is generated and analyzed. Figure 10 illustrates 3D and 2D examples on how the Pareto fronts are interpreted. Here, the red and green colors represent the highest and lowest T_{o_s} and small and large grey color represents the lowest and highest $T_{o_{win}}$. The X axis is cooling load in warm months, Y axis is heating load in cold months and Z axis is sum of TDT in both summer and winter. The most optimum solutions should occur near coordinate origin (0,0,0) or inside the region is marked with red dashed-line in Figure 10-a. Figure 10-b shows a 2D trade-off Pareto front between the cooling and heating loads and possible best solutions (non-dominated solutions), dominated solutions and single objective optimal solutions.

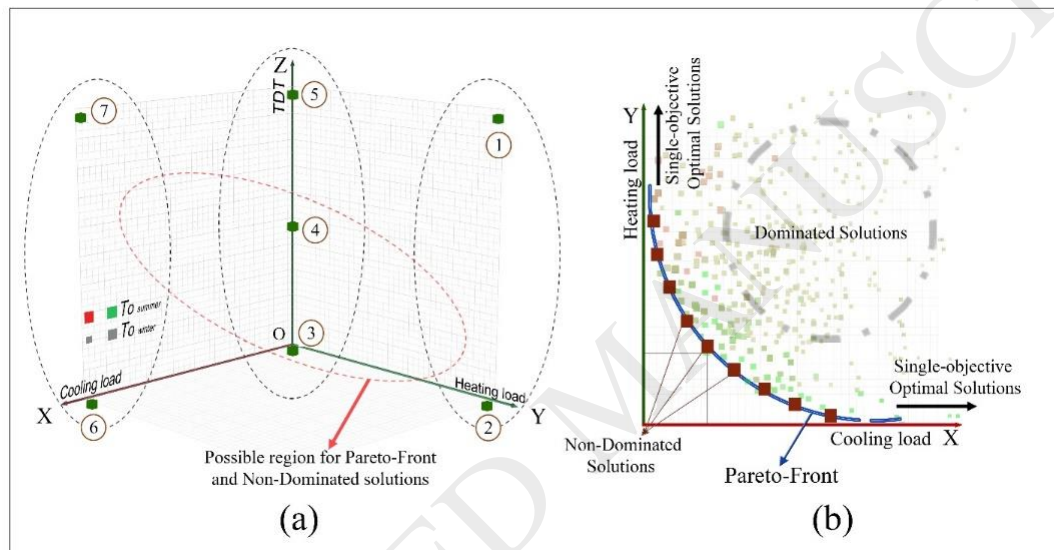


Figure 10. (a) 3D Pareto front interpretation: Possible results for: (1) and (2) Minimum cooling load solutions, (3) Origin (0,0,0) with best design solutions considering all objectives, (4) Nearly optimal solutions considering all objectives, (5) Maximum TDT solutions, (6) and (7) Minimum heating load solutions. (b) 2D trade-off between cooling and heating load, non-dominated solutions and Pareto-Front

3. Results and discussions

The Pareto-Fronts of five main optimization problems for similar BMC and UD are illustrated in Figure 11 and results for other optimization problems are discussed in six main sub-sections based on UDs, BMCs and five introduced objectives (q_c , q_h , TDT, T_{o_s} and $T_{o_{win}}$). Moreover, the layouts of best non-dominated solutions in each urban area are extracted out of the optimization process. In the other words, 1998 non-dominated solutions were ranked based on the results of introduced functions and top hundred form combinations with minimum energy demand and TDT while maintain T_{o_s} and $T_{o_{win}}$ in the defined comfort zone (Figure 12). Here, only the layouts of twenty best design solutions are selected to represent all optimal solutions in order to limit the size of the paper. Thus, eight solutions with similar BMC and UD (for example Max BMC in Max UD) and three solutions for other four BMCs in the same UD (best cooling demand, best heating demand and best annual energy demand) are presented. Figure A.2 in Appendix A show the

boxplots and annual hourly energy demand of eight solutions with similar BMC and UD. At the final step (Section 3.6) the main design-aid recommendations based on the analysis of the layout and the form of all the best combinations are discussed. At the end, a summary of characteristics for the best design solutions is presented in Table 2, which can be used by designers as a form-finding role of thumbs.

3.1 Urban area with MaxUD

Twenty-best design solutions out of 207 non-dominated solutions in MaxUD are illustrated in Figure 12-a. Results of MaxUD showed that variations of cooling and heating demand (Figure 13-a and 14-a), TDT and T_o (Figure 15-a) are up to 6.2 kWh/m², 22.4 kWh/m², 12.2% and 1.6°C respectively. These variations can indicate the importance of introduced form indicators on thermal performance of buildings. Generated forms with Min BMC had the highest cooling and heating demand (5.1 kWh/m² and 25.9 kWh/m² respectively) compared to cases with Mean BMC (with about 20% lower energy demand); the higher BMC results in lower energy demand. A deeper look into the best design solutions shows that 68% of them have at least one or two empty cells on north/south elevation. Moreover, 54% of the best design solutions have at least two or more adjacent empty cells on western elevation; where induce higher thermal circulation by working as openings in building sides located in dense areas and increase the natural convection of air in the northern and southern canopies. About 64% of solutions have set-backs toward the northern side of the site which enables more efficient solar gain in cold seasons and facilitating scheduled ventilation through openings and higher wind speed at the hatches of air-conditioner systems in warm seasons. Furthermore, courtyard/semi-courtyard forms (CY) with 59% of the solutions are the most frequent building form. Finally, 61% of the solutions in MaxUD have 75-degree clockwise site rotation with 345-255 horizontal axis which enables a larger part of the target building to face northern elevation with no surrounding buildings and obstacles (Figure 15-g).

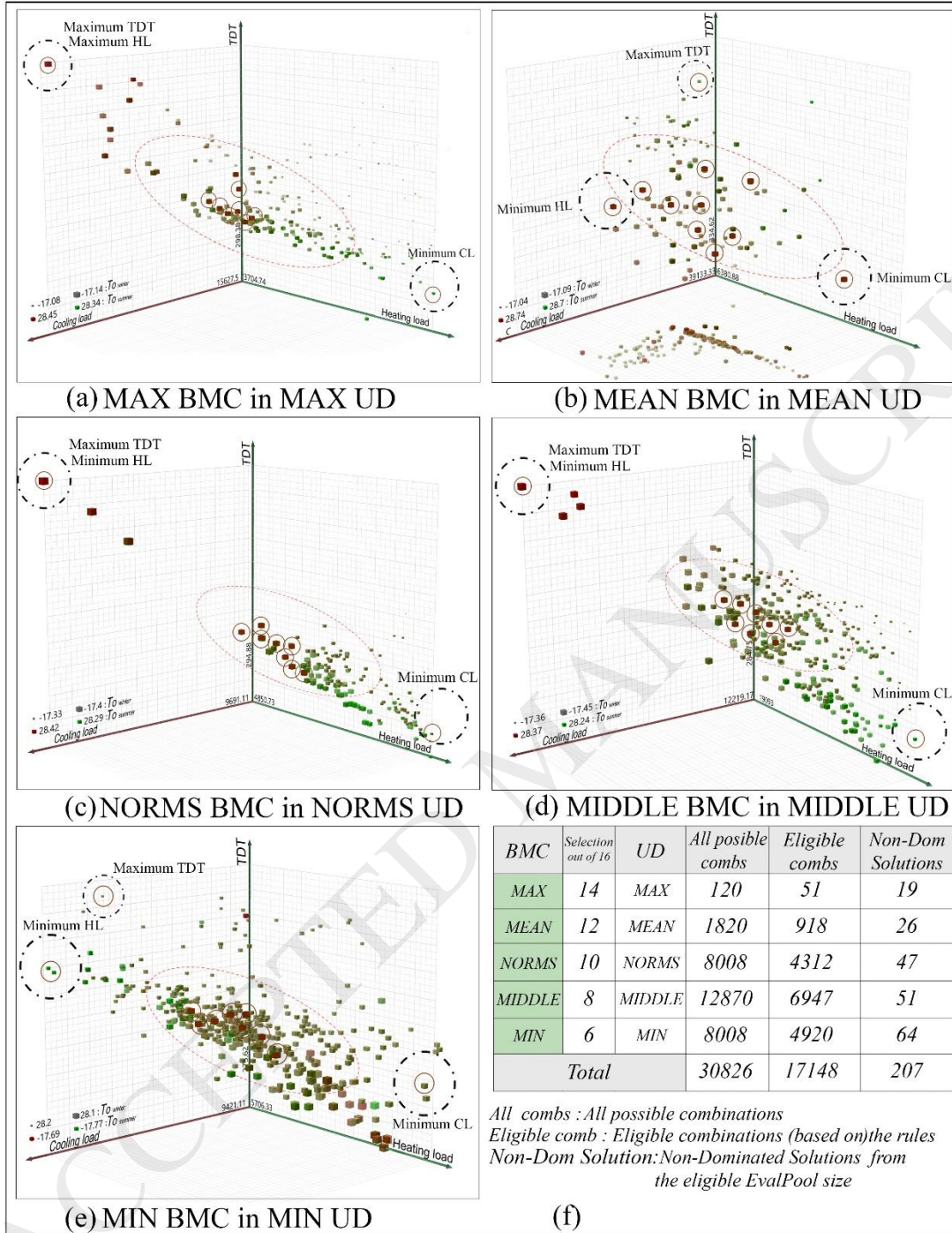


Figure 11. Pareto-Front of five main category of the defined optimization problems: (a) Max BMC in MAXUD, (a) Mean BMC in MEANUD, (a) Norms BMC in NORMSUD, (a) Middle BMC in MIDDLEUD, (a) Min BMC in MINUD, (f) the statistics of five main optimization problems based on similar UD and BMC.





Figure 12. 100 best design solutions based on each UD: (a) MaxUD, (b) MeanUD, (c) NormsUD, (d) MiddleUD, (e) MinUD

3.2 Urban area with MeanUD

Figure 12-b shows twenty-best design solutions with all BMCs in MeanUD; where form combinations with Mean BMC have 35% (2.2 kWh/m²) lower cooling and 17% (4.2 kWh/m²) lower heating demand. Moreover, cooling and heating demand (Figure 13-b and 14-b), TDT and T_o (Figure 15-b) variations among all eligible combinations can vary up to 8.2 kWh/m², 11.3 kWh/m², 8.2% and 1.1 °C respectively. An overview of 210 best design solutions with five BMCs in MeanUD shows that about 48% of them have at least one empty cell (semi-courtyard form) in a part of an integrated layout, and 23% have L forms and 18% U forms. In terms of lower heating demand, more than 78% of the solutions have CY or semi-CY forms. Interestingly, about 77% of the best design solutions in terms of heating demand have set-backs to the northern side of the site. Furthermore, 40% of the best solutions in MaxUD urban area had 75-degree clockwise site rotation and 29% had 90-degree clockwise site rotation which enables a larger part of the target building to face northern elevation with no surrounding buildings (Figure 15-h).

3.3 Urban area with NormsUD

The layouts of twenty-best design solutions in NormsUD are rendered in Figure 12-c. Here, the combinations with Max BMC have about 33% and 17% lower cooling and heating demand (1.6 kWh/m^2 and 4.3 kWh/m^2) compared to cases with Min BMC. The Cooling and heating demand (Figure 13-c and 14-c), TDT and T_o (Figure 15-c) variations among eligible combinations are up to 11.1 kWh/m^2 , 26.2 kWh/m^2 , 7% and 1.2°C respectively. Considering 210 best design solutions with five BMCs, 61% of them have at least one empty cell in a part of a uniform layout (semi-courtyard form). However, in terms of optimal heating demand design solutions more than 86% of the best solutions have CY or semi-CY forms. Moreover, 91% of the best solutions have at least two or more empty cells in western and northern sides. In terms of heating demand, about 84% of them have set-backs to the northern side of the site. Furthermore, 78% of them in NormsUD urban area have 75-degree clockwise site rotation, enabling a larger part of the target building to face northern elevation with no surrounding buildings (Figure 15-i).

3.4 Urban area with MiddleUD

Figure 12-d illustrates twenty-best design solutions in MiddleUD; in which cases with Max BMC with the lowest energy demand have about 27% (1.6 kWh/m^2) and 10% (2.7 kWh/m^2) lower cooling and heating demand compared to Min BMC. In MiddleUD, up to 7.1 kWh/m^2 and 24.3 kWh/m^2 cooling and heating demand (Figure 13-d and 14-d); 5.2% TDT and 0.93°C T_o (Figure 15-d) variations noticed among eligible combinations. About 41% of the solutions have at least one empty cell as a courtyard form in an integrated plan. In terms of optimal heating demand, more than 65% of the best solutions have CY or semi-CY form; where 68% of those forms have set-backs to the northern side of the site. About 74% of non-dominated solutions have at least two or more empty cells in the western and northern sides. Finally, 60% of the best solutions in MiddleUD urban area have 75-degree clockwise site rotation and 20% have 90-degree clockwise site rotation, which enables a larger part of the target building to face northern elevation with no surrounding buildings (Figure 15-j).

3.5 MIN Urban Density

Twenty-best design solutions of BMCs in MinUD are presented in Figure 12-e. Results showed that cooling and heating demand (Figure 13-e and 15-e), TDT and T_o (Figure 15-e) variations are up to 10.8 kWh/m^2 , 24.2 kWh/m^2 , 5.1% and 0.76°C respectively. Similar to the Middle UD and NormsUD, combinations with Max BMC in MinUD have about 26% (1.7 kWh/m^2) cooling and 8% (2 kWh/m^2) heating demand compared to Min BMC's cases. Here, 60% have at least one empty cell (semi-courtyard form) in a part of integrated layout and 18% have L or U forms. In terms of optimal heating demand design solutions more than 72% of the best solutions have semi-CY form and 48% have set-backs to the northern side of the site. Around 74% of the best solutions have 90-degree clockwise site rotation and 18% had 75-degree clockwise site rotation (Figure 15-k).

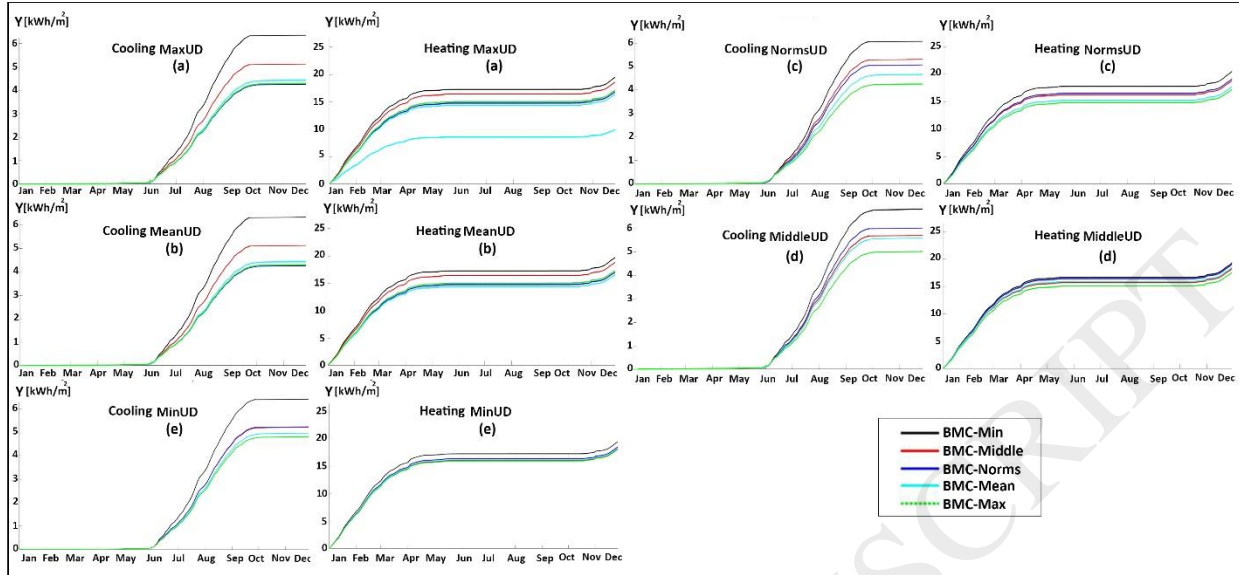


Figure 13. Average annual cumulative energy demand: (a) MaxUD, (b) MeanUD, (c) NormsUD, (d) MiddleUD, (e) MinUD

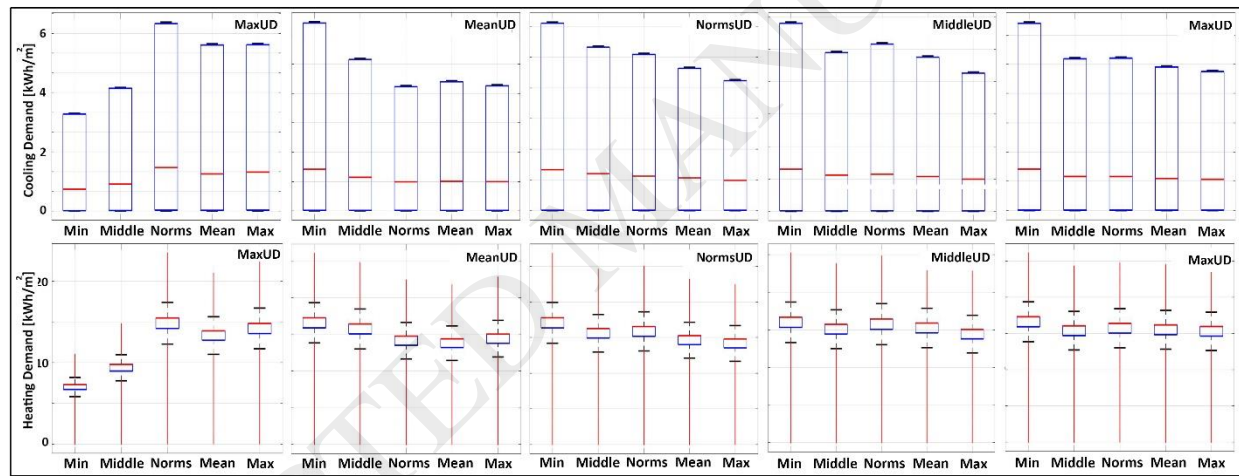


Figure 14. Boxplot of energy demand for BMCs in each UD (a) MaxUD, (b) MeanUD, (c) NormsUD, (d) MiddleUD, (e) MinUD

3.6. Step 4: Form-Solutions

In the final step of the EEF framework, a series of design-based suggestions for architects and urban designers out of 1998 best design solutions are presented for real applications as optimal solutions for having the minimum possible energy demand, TDT and T_o . These suggestions can be adopted by designers in similar contexts and climates; however, it is recommended to assign EEF framework for each design problem by the design team. According to the results of twenty-five optimization studies, in terms of optimal cooling and heating demand, 62% of the generated form combinations have courtyard or semi-courtyard forms, 21% have L or U forms and the rest or particular single forms from T form to distinct subtractive forms; while for the optimal heating demand more than 73% of combinations have CY or semi-CY forms in all UD with any type of BMC.

In terms of TDT and T_o , semi-CY forms are also the most frequent solutions with more than 60%. Considering all objectives, semi-CY and U forms are the most frequent optimal form combinations. A reason for the high number of CY or semi-CY forms in the best solutions is the higher temperature in the courtyard in winters (0.9 to 1.4 C) and respectively lower temperature in summers (2.9 to 3.8 C) compare to calculated temperature of the surrounding spaces. Among the solutions, 66% have entire or at least one joint-part with a cuboid geometry and 71% are recessed to the northern side of the site. Cuboid geometry with set-backs to the north enable higher solar radiation in the northern side of the building in the cold months. Another interesting fact is the frequency of empty cells in the western and southern sides of optimal solutions in almost all BMCs in every UD. Empty cells have a considerable impact on temperature variation around and inside adjacent building cells; a reason is higher external surface to gain solar heat. Furthermore, a clear trend was noticed in the relation of UDs and BMCs; where in denser urban areas, the variation of BMC has a considerable higher impact on cooling and heating demand and thermal comfort indicators. For example, in MaxUD and MeanUD areas, combinations with Mean and Max BMC have the most optimal solutions.

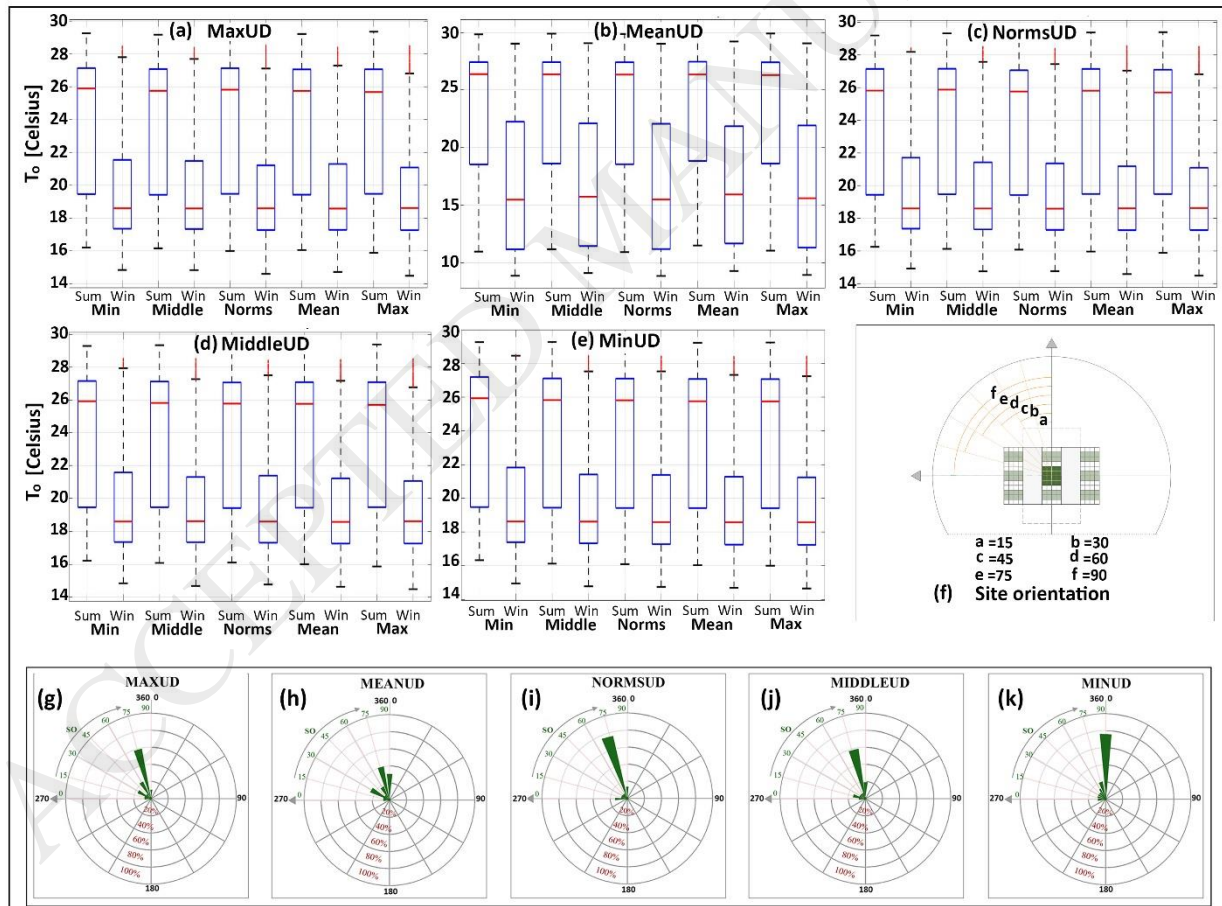


Figure 15. Boxplot of average T_o for all BMC in each UD in cold and warm seasons: (a) MaxUD, (b) MeanUD, (c) NormsUD, (d) MiddleUD, (e) MinUD, (f) diagram of site orientation angles applied as a genome into the main optimization process, Site orientation frequency of the best design solutions in the defined urban areas: (g) MaxUD, (h) MeanUD, (i) NormsUD, (j) MiddleUD, (k) MinUD

In other urban areas with lower UD (under 60%), form combinations with Max BMC have the most frequent optimal solutions. It can be concluded that higher BMC results in lower energy demand per square meter and more optimal thermal comfort indicators accordingly; particularly in dense urban areas. In addition to the role of BMC, the layout and geometry of generated combinations are other important parameters. Thus, it is important to consider all building's design techniques such as mass and void in layout and form, set-backs, height variations and orientations according to the values of the investigated objectives. For instance, in terms of site orientation, about 46% and 31% of all 1998 solutions had 75 and 90-degree clock-wise orientation respectively. The most frequent site orientation in MaxUD, NormsUD, MiddleUD and MinUD was 75-degree. However, in Mean BMC 45% optimal solutions had 90-degree orientation angle. The summary of design-aid suggestions based on UD and BMC are presented in Table 2 and some notable design-aid suggestions can be categorized based on the defined urban morphology and site boundaries as follows:

It is recommended to:

- Design overall form of buildings based on a semi-U or semi-CY layout with Rc (Figure 2-n) higher than 0.75-0.89 (the Rc of a cube is 1) in areas with Norms, Mean and MaxUD (dense urban areas). Design overall form of buildings based on a semi-CY and semi-L layout with Rc between 0.85 to 0.98 in areas with Middle and MinUD (urban areas with low density).
- Rotate the form of the building up to 15-degree clock-wise on the northern-southern axis (placing the form on NW/SE axis) in areas with Norms, Mean and MaxUD. In other words, in dense urban areas the main axis of the building's layout should face Northwest. This will provide higher solar radiation in winter and higher ventilation in summer.
- Considering a high angle of rotation for building in areas with Middle and MinUD (in some cases between 15 to 60-degree clock-wise on the northern-southern axis). In these urban areas further investigation is required to determine the form orientation due to higher accessibility to solar radiation and wind flow.
- Design overall form of buildings close to semi-CY layout to have the highest heating demand reduction almost in all form combinations. The semi-CY layout design is traditionally one of the most frequent building forms in the regions with hot-arid climate in Iran. A high number of semi-CY forms showed cooling demand reduction as well. The final form can include a non-closed courtyard.
- Consider set-backs toward northern boundaries of the site in order to gain more solar radiation through openings for almost all forms in different urban areas. Although in the case of set-backs separate analysis is suggested for each project, moving the overall form of the building to the northern boundaries of the site showed a significant energy demand reduction, particularly during cold season (heating demand).
- Split the western side of the building's form and consider mass pull and push in the layout (step-like design) to reduce surfaces with openings facing west. With this envelope fold-strategy a higher total area of the building can face North/South which results in lower energy demand in almost all urban areas.

It is not recommended to:

- Design unified forms with built density lower than 50% (Middle BMC) in almost all urban areas. It may result in higher energy demand in most cases with some exceptions, however for non-unified and detached forms in a site, the results may differ.
- Considering set-back of the forms to the southern side of the site (with few exceptions, none of the best design solutions have this kind of situation). In these cases, a large part of the southern elevation of the buildings were blocked by the adjacent buildings, particularly in the dense urban areas.
- Design central courtyards or open spaces on the northern boundary of the site. These spaces should be placed with at least one cell distance from the ultimate northern boundary of site to gain higher solar radiation in cold months. This can provide higher solar radiation for the remaining cell. Otherwise, the overall form of the building will be semi-U facing the north; which a limited number of the best solutions have such a condition.
- Design building forms with R_c lower than 0.7 in urban areas (it is important to design forms with similar total area with high R_c close to 1). In other words, the overall form of the building should be close to cube/cuboid while according to results, a high number of best solutions had cuboid forms.
- Exclude small open spaces in the southern and eastern boundaries of the site in urban areas with high urban density. In the dense urban areas, small open spaces in the southern and eastern sides of the site provide higher shading in the warm seasons which results in lower cooling demand and higher thermal comfort. Consider high angles of rotation for the overall form of buildings in almost all urban areas with typical urban density. However, for cases placed in areas with low urban density, buildings can have up to 75-degree rotation in some particular conditions (further investigations is required for such situations).

Several variables in this study were considered as constant values based on dozens of sensitivity analyses and the national construction codes of Tehran to focus on the overall form of buildings. These parameters and variables can be manually remodified based on the constraints of each real design projects. This also helped to limit the calculation loads and consequently lower process time. This study adopted five detailed urban models to include the impacts of urban morphology of Tehran in the energy demand and thermal comfort calculations. The considered urban areas in this research (each with 24000 m² total area) only represent microscale neighbourhoods of Tehran with simplified geometries. However, several influencing parameters have been taken into account to consider the design-based aspects of each urban model by evaluating 1600 urban morphologies according to an earlier work [98] . Moreover, the form combinations were defined based on a rectangular grid. This means that more complex forms and circular geometries cannot be included in the Form-Generation step. To minimize the impact of this limitation, several flexible geometric constraints were defined to control the form of the building a wide range of frequent forms were considered in the optimization process. The generated forms cover the majority of frequent office building forms in Tehran based on building codes and construction trends. However, further investigation is still required to include more complex forms (forms with circular spaces in the layout) or more variations in the final height.




















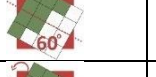

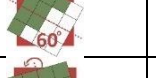
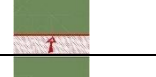
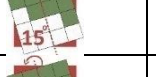


4. Conclusions

A multi-objective optimization framework was introduced for form finding process in early stage design in this study, namely Energy Efficient Form-finder (EEF) for high-rise office buildings. The procedure contained four steps, including Form-Generation, Form-Simulation, Form-Optimization and Form-Solutions based on a Grasshopper algorithm platform. A novel approach adopted developing a new technique namely “Building Modular Cell” (BMC) to generate accurate and realistic urban and building models in GH algorithm with a series of geometric constraints. Then, simulation engines were defined in the algorithm to calculate cooling and heating demand, Thermal Discomfort Time (TDT) and Operative Temperature (T_o) of each form combination. In the next step, twenty-five optimization problems were studied based on UD of urban areas and BMC of the reference buildings. After thousands of iterations, 1998 non-dominated solutions selected as the “best design solutions” out of 85740 eligible combinations (eligible generated forms are based on the mathematical combinations of the cells according to a series of form generation rules as design constraints). Finally, the qualitative and quantitative results of twenty-five optimization problems were discussed and presented in a comprehensive table. According to the result, by adopting EEF, the energy demand of generated forms can be reduced notably while maintaining thermal comfort.

By adopting EEF framework, cooling and heating demand and TDT of high-rise office buildings can be reduced for more than 35% (2.2 kWh/m²), 17% (5 kWh/m²) and 12.2% respectively while maintaining T_o in both warm and cold months in the defined comfort zone based on ASHRAE 55. Considering all eligible combinations, this reduction is considerably higher (11.1 kWh/m² cooling and 26.2 kWh/m² heating demand) which indicates the impact of EEF in the form-finding process. Moreover, courtyard and semi-courtyard forms were the most frequent forms in optimal solutions in all the urban areas; particularly in terms of heating demand. The majority of the best solutions had set-backs toward northern side of the sub-site of reference building; while the highest number of empty cells occurred in western side of generated combinations. The most frequent site orientation's angles were 75 and 90 degrees (15-degree clock-wise rotation or design according to northern-southern axis for the main building. Finally, based on the main findings of the study, a series of unique design-aid recommendations and a summary table (Table 2) were derived out of the layouts and geometry of all non-dominated solutions, which can be adopted in real practice by engineers, architects and urban designers in Form-Solution step as role of thumb.

Table 2. Design-based suggestions derived out of 1998 non-dominated solutions from all BMCs and UD

Urban areas	BMC	Best combination forms										
		Rc	Energy reduction	Demand	Frequent	CD	HD	Set-back	Empty cell	Building rotation	Solar gain axis	
MaxUD	Max	0.89	9%		U, CY, L	U, CY	CY	-				NW/SE
	Mean	0.80	30%		CY, U, L	U, CY	CY				NW/SE	
	Norms	0.89	28%		CY, L, C	U	CY				NW/SE	
	Middle	0.77	21%		CY, U, W	L, C	CY				NW/SE	
	Min	0.85	5%		L, U, T	L	CY				NW/SE	
MeanUD	Max	0.89	33%		CY, L, C	U, CY	CY	-				NW/SE
	Mean	0.73	30%		L, CY, U	U, CY	CY				NW/SE	
	Norms	0.71	23%		CY, U, C	U	CY				NW/SE	
	Middle	0.68	18%		CY, L, C	L	CY				NW/SE	
	Min	0.72	9%		L, T, U	L, T	CY				NW/SE	
NormsUD	Max	0.98	30%		CY, U, L	U, CY	CY	-				NW/SE
	Mean	0.91	24%		U, CY, L	U, CY	CY				NE/Sw	
	Norms	0.79	20%		CY, L, U	U, C	CY				NW/SE	

	Middle	0.80	16%	L, U, C	L	CY				NW/SE
	Min	0.72	12%	L, C, U	L	CY				NW/SE
MiddleUD	Max	0.97	26%	L, C, CY	U, CY	CY	-			NW/SE
	Mean	0.83	22%	CY, C, U	U, CY	CY			NW/SE	
	Norms	0.71	17%	CY, L, U	U, C	CY			NW/SE	
	Middle	0.69	13%	CY, U, C	L, CY	CY			NW/SE	
	Min	0.72	8%	L, U, C	L	CY			NW/SE	
MinUD	Max	0.89	25%	CY, C	U, CY	CY	-			NW/SE
	Mean	0.73	21%	CY, U, C	U, CY	CY			NW/SE	
	Norms	0.65	16%	CY, U, C	U, C	CY			NW/SE	
	Middle	0.70	11%	CY, L, C	L	CY			NW/SE	
	Min	0.73	7%	L, U, C	L	CY			NW/SE	

This study provided further evidence on the importance of adopting multi-objective optimization framework in the early design stages for form finding process, which results in taking low-cost design-solutions. The introduced framework and unique techniques in this work, has shorten the form finding process time for simulation and optimization while enhance the accuracy of the assessment by considering several parameters and indicators for defining the overall form of buildings. The design-based origin of EEF enables designers to follow the form finding process of an energy efficient building; in parallel with their architectural concepts and thoughts of their design problem at early stages. Moreover, developed Grasshopper (GH) algorithm is user-friendly and easily can be adopted for new design projects by changing the properties of considered parameters and constraints (such as urban areas, construction materials, building height, etc.), grid resolution and climatic data. On the other hand, by the same workflow and structure, other visual parametric tools such as Dynamo can be used to run the EEF. Finally, the database of results is applicable for developing new building codes and regulations in Tehran or any other dense cities with similar conditions. As future research, further investigations to develop the EEF into an easy-to-setup plugin in Grasshopper is targeted which can provide more detailed urban areas and microclimate. Moreover, developing an adjustable triangular grid to consider more complex forms with non-rectangular geometry into the EEF can be another step to enable more freedom for designers.

Acknowledgement

This work has partly benefited from the support of the Swedish Research Council (Formas) which is gratefully acknowledged.

References

- [1] World Urbanization Prospects - Population Division - United Nations n.d. <https://esa.un.org/unpd/wup/> (accessed May 18, 2018).
- [2] Cohen B. Urbanization in developing countries: Current trends, future projections, and key challenges for sustainability. *Technology in Society* 2006;28:63–80. doi:10.1016/j.techsoc.2005.10.005.
- [3] Srebric J, Heidarinejad M, Liu J. Building neighborhood emerging properties and their impacts on multi-scale modeling of building energy and airflows. *Building and Environment* 2015;91:246–62. doi:10.1016/j.buildenv.2015.02.031.
- [4] Fifth Assessment Report - Mitigation of Climate Change. Cambridge University Press; n.d.
- [5] Ruparathna R, Hewage K, Sadiq R. Improving the energy efficiency of the existing building stock: A critical review of commercial and institutional buildings. *Renewable and Sustainable Energy Reviews* 2016;53:1032–45. doi:10.1016/j.rser.2015.09.084.
- [6] Antoniadou P, Papadopoulos AM. Occupants' thermal comfort: State of the art and the prospects of personalized assessment in office buildings. *Energy and Buildings* 2017;153:136–49. doi:10.1016/j.enbuild.2017.08.001.
- [7] Griego D, Krarti M, Hernandez-Guerrero A. Energy efficiency optimization of new and existing office buildings in Guanajuato, Mexico. *Sustainable Cities and Society* 2015;17:132–40. doi:10.1016/j.scs.2015.04.008.
- [8] Nik VM. Making energy simulation easier for future climate – Synthesizing typical and extreme weather data sets out of regional climate models (RCMs). *Applied Energy* 2016;177:204–26. doi:10.1016/j.apenergy.2016.05.107.
- [9] Moazami A, Nik VM, Carlucci S, Geving S. Impacts of future weather data typology on building energy performance – Investigating long-term patterns of climate change and extreme weather conditions. *Applied Energy* 2019;238:696–720. doi:10.1016/j.apenergy.2019.01.085.
- [10] Gaonkar P, Bapat J, Das D. Location-aware multi-objective optimization for energy cost management in semi-public buildings using thermal discomfort information. *Sustainable Cities and Society* 2018;40:174–81. doi:10.1016/j.scs.2017.12.021.
- [11] Nik VM, Sasic Kalagasidis A. Impact study of the climate change on the energy performance of the building stock in Stockholm considering four climate uncertainties. *Building and Environment* 2013;60:291–304. doi:10.1016/j.buildenv.2012.11.005.
- [12] Kalnay E, Cai M. Impact of urbanization and land-use change on climate. *Nature* 2003;423:528–31. doi:10.1038/nature01675.
- [13] Global and European temperature. European Environment Agency n.d. <https://www.eea.europa.eu/data-and-maps/indicators/global-and-european-temperature/global-and-european-temperature-assessment-5> (accessed July 16, 2018).
- [14] Perera ATD, Nik VM, Mauree D, Scartezzini J-L. An integrated approach to design site specific distributed electrical hubs combining optimization, multi-criterion assessment and decision making. *Energy* 2017;134:103–20. doi:10.1016/j.energy.2017.06.002.
- [15] Perera ATD, Nik VM, Mauree D, Scartezzini J-L. Electrical hubs: An effective way to integrate non-dispatchable renewable energy sources with minimum impact to the grid. *Applied Energy* 2017;190:232–48. doi:10.1016/j.apenergy.2016.12.127.

- [16] Mahdavinejad M, Javanroodi K. Natural ventilation performance of ancient wind catchers, an experimental and analytical study - case studies: one-sided, two-sided and four-sided wind catchers. *International Journal of Energy Technology and Policy* 2014;10:36. doi:10.1504/IJETP.2014.065036.
- [17] Pourazarm E, Cooray A. Estimating and forecasting residential electricity demand in Iran. *Economic Modelling* 2013;35:546–58. doi:10.1016/j.econmod.2013.08.006.
- [18] Bagheri F, Mokarizadeh V, Jabbar M. Developing energy performance label for office buildings in Iran. *Energy and Buildings* 2013;61:116–24. doi:10.1016/j.enbuild.2013.02.022.
- [19] Annual Energy Fact Sheet report 2015. Iran Energy Efficiency Organization; 2015.
- [20] Ghasemi AR. Changes and trends in maximum, minimum and mean temperature series in Iran. *Atmospheric Science Letters* n.d.;16:366–72. doi:10.1002/asl2.569.
- [21] National Building Codes of Iran No.19. Tehran: Construction Engineering Organization; 2009.
- [22] Rohdin P, Molin A, Moshfegh B. Experiences from nine passive houses in Sweden – Indoor thermal environment and energy use. *Building and Environment* 2014;71:176–85. doi:10.1016/j.buildenv.2013.09.017.
- [23] Gou S, Nik VM, Scartezzini J-L, Zhao Q, Li Z. Passive design optimization of newly-built residential buildings in Shanghai for improving indoor thermal comfort while reducing building energy demand. *Energy and Buildings* 2018;169:484–506. doi:10.1016/j.enbuild.2017.09.095.
- [24] Verbeke S, Audenaert A. Thermal inertia in buildings: A review of impacts across climate and building use. *Renewable and Sustainable Energy Reviews* 2018;82:2300–18. doi:10.1016/j.rser.2017.08.083.
- [25] Longo S, Montana F, Riva Sanseverino E. A review on optimization and cost-optimal methodologies in low-energy buildings design and environmental considerations. *Sustainable Cities and Society* 2019;45:87–104. doi:10.1016/j.scs.2018.11.027.
- [26] Nguyen A-T, Reiter S, Rigo P. A review on simulation-based optimization methods applied to building performance analysis. *Applied Energy* 2014;113:1043–58. doi:10.1016/j.apenergy.2013.08.061.
- [27] Baños R, Manzano-Agugliaro F, Montoya FG, Gil C, Alcayde A, Gómez J. Optimization methods applied to renewable and sustainable energy: A review. *Renewable and Sustainable Energy Reviews* 2011;15:1753–66. doi:10.1016/j.rser.2010.12.008.
- [28] Delgarm N, Sajadi B, Kowsary F, Delgarm S. Multi-objective optimization of the building energy performance: A simulation-based approach by means of particle swarm optimization (PSO). *Applied Energy* 2016;170:293–303. doi:10.1016/j.apenergy.2016.02.141.
- [29] Selakov A, Cvijetinović D, Milović L, Mellon S, Bekut D. Hybrid PSO–SVM method for short-term load forecasting during periods with significant temperature variations in city of Burbank. *Applied Soft Computing* 2014;16:80–8. doi:10.1016/j.asoc.2013.12.001.
- [30] Socha K, Dorigo M. Ant colony optimization for continuous domains. *European Journal of Operational Research* 2008;185:1155–73. doi:10.1016/j.ejor.2006.06.046.
- [31] Bamdad K, Cholette ME, Guan L, Bell J. Ant colony algorithm for building energy optimisation problems and comparison with benchmark algorithms. *Energy and Buildings* 2017;154:404–14. doi:10.1016/j.enbuild.2017.08.071.

- [32] Delgarm N, Sajadi B, Delgarm S, Kowsary F. A novel approach for the simulation-based optimization of the buildings energy consumption using NSGA-II: Case study in Iran. *Energy and Buildings* 2016;127:552–60. doi:10.1016/j.enbuild.2016.05.052.
- [33] Magnier L, Haghghat F. Multiobjective optimization of building design using TRNSYS simulations, genetic algorithm, and Artificial Neural Network. *Building and Environment* 2010;45:739–46. doi:10.1016/j.buildenv.2009.08.016.
- [34] Li H, Nalim R, Haldi P-A. Thermal-economic optimization of a distributed multi-generation energy system—A case study of Beijing. *Applied Thermal Engineering* 2006;26:709–19. doi:10.1016/j.applthermaleng.2005.09.005.
- [35] Ascione F, Bianco N, De Masi RF, De Stasio C, Mauro GM, Vanoli GP. Multi-objective optimization of the renewable energy mix for a building. *Applied Thermal Engineering* 2016;101:612–21. doi:10.1016/j.applthermaleng.2015.12.073.
- [36] Perera DWU, Winkler D, Skeie N-O. Multi-floor building heating models in MATLAB and Modelica environments. *Applied Energy* 2016;171:46–57. doi:10.1016/j.apenergy.2016.02.143.
- [37] Carlucci S, Pagliano L, Zangheri P. Optimization by Discomfort Minimization for Designing a Comfortable Net Zero Energy Building in the Mediterranean Climate. *Advanced Materials Research* 2013. doi:10.4028/www.scientific.net/AMR.689.44.
- [38] Bigot D, Miranville F, Boyer H, Bojic M, Guichard S, Jean A. Model optimization and validation with experimental data using the case study of a building equipped with photovoltaic panel on roof: Coupling of the building thermal simulation code ISOLAB with the generic optimization program GenOpt. *Energy and Buildings* 2013;58:333–47. doi:10.1016/j.enbuild.2012.10.017.
- [39] Jedrzejuk H, Marks W. Optimization of shape and functional structure of buildings as well as heat source utilisation example. *Building and Environment* 2002;37:1249–53. doi:10.1016/S0360-1323(01)00100-7.
- [40] Marks W. Multicriteria optimisation of shape of energy-saving buildings. *Building and Environment* 1997;32:331–9. doi:10.1016/S0360-1323(96)00065-0.
- [41] Lee B, Trcka M, Hensen JLM. Building energy simulation and optimization: A case study of industrial halls with varying process loads and occupancy patterns. *Build Simul* 2014;7:229–36. doi:10.1007/s12273-013-0154-3.
- [42] Shi X. Design optimization of insulation usage and space conditioning load using energy simulation and genetic algorithm. *Energy* 2011;36:1659–67. doi:10.1016/j.energy.2010.12.064.
- [43] Asadi E, da Silva MG, Antunes CH, Dias L. A multi-objective optimization model for building retrofit strategies using TRNSYS simulations, GenOpt and MATLAB. *Building and Environment* 2012;56:370–8. doi:10.1016/j.buildenv.2012.04.005.
- [44] Asadi E, Silva MG da, Antunes CH, Dias L, Glicksman L. Multi-objective optimization for building retrofit: A model using genetic algorithm and artificial neural network and an application. *Energy and Buildings* 2014;81:444–56. doi:10.1016/j.enbuild.2014.06.009.
- [45] Ascione F, Bianco N, De Stasio C, Mauro GM, Vanoli GP. Simulation-based model predictive control by the multi-objective optimization of building energy performance and thermal comfort. *Energy and Buildings* 2016;111:131–44. doi:10.1016/j.enbuild.2015.11.033.

- [46] Camporeale PE, Mercader Moyano M del P, Czajkowski JD. Multi-objective optimisation model: A housing block retrofit in Seville. *Energy and Buildings* 2017;153:476–84. doi:10.1016/j.enbuild.2017.08.023.
- [47] Jin J-T, Jeong J-W. Optimization of a free-form building shape to minimize external thermal load using genetic algorithm. *Energy and Buildings* 2014;85:473–82. doi:10.1016/j.enbuild.2014.09.080.
- [48] Østergård T, Jensen RL, Maagaard SE. Building simulations supporting decision making in early design – A review. *Renewable and Sustainable Energy Reviews* 2016;61:187–201. doi:10.1016/j.rser.2016.03.045.
- [49] Zhou Z, Wang C, Sun X, Gao F, Feng W, Zillante G. Heating energy saving potential from building envelope design and operation optimization in residential buildings: A case study in northern China. *Journal of Cleaner Production* 2018;174:413–23. doi:10.1016/j.jclepro.2017.10.237.
- [50] Song X, Ye C, Li H, Wang X, Ma W. Field study on energy economic assessment of office buildings envelope retrofitting in southern China. *Sustainable Cities and Society* 2017;28:154–61. doi:10.1016/j.scs.2016.08.029.
- [51] Cascone Y, Capozzoli A, Perino M. Optimisation analysis of PCM-enhanced opaque building envelope components for the energy retrofitting of office buildings in Mediterranean climates. *Applied Energy* 2018;211:929–53. doi:10.1016/j.apenergy.2017.11.081.
- [52] Morini E, Castellani B, Anderini E, Presciutti A, Nicolini A, Rossi F. Optimized retro-reflective tiles for exterior building element. *Sustainable Cities and Society* 2018;37:146–53. doi:10.1016/j.scs.2017.11.007.
- [53] Dombaycı ÖA, Gölcü M, Pancar Y. Optimization of insulation thickness for external walls using different energy-sources. *Applied Energy* 2006;83:921–8. doi:10.1016/j.apenergy.2005.10.006.
- [54] Jin Q, Favoino F, Overend M. Design and control optimisation of adaptive insulation systems for office buildings. Part 2: A parametric study for a temperate climate. *Energy* 2017;127:634–49. doi:10.1016/j.energy.2017.03.096.
- [55] Fernández E, Beckers B, Besuievsky G. A fast daylighting method to optimize opening configurations in building design. *Energy and Buildings* 2016;125:205–18. doi:10.1016/j.enbuild.2016.05.012.
- [56] Amaral AR, Rodrigues E, Gaspar AR, Gomes Á. A thermal performance parametric study of window type, orientation, size and shadowing effect. *Sustainable Cities and Society* 2016;26:456–65. doi:10.1016/j.scs.2016.05.014.
- [57] Yi YK, Yin J, Tang Y. Developing an advanced daylight model for building energy tool to simulate dynamic shading device. *Solar Energy* 2018;163:140–9. doi:10.1016/j.solener.2018.01.082.
- [58] Moghadam H, Deymeh SM. Determination of optimum location and tilt angle of solar collector on the roof of buildings with regard to shadow of adjacent neighbors. *Sustainable Cities and Society* 2015;14:215–22. doi:10.1016/j.scs.2014.09.009.
- [59] Ge J, Wu J, Chen S, Wu J. Energy efficiency optimization strategies for university research buildings with hot summer and cold winter climate of China based on the adaptive thermal comfort. *Journal of Building Engineering* 2018;18:321–30. doi:10.1016/j.jobeb.2018.03.022.

- [60] Eskander MM, Sandoval-Reyes M, Silva CA, Vieira SM, Sousa JMC. Assessment of energy efficiency measures using multi-objective optimization in Portuguese households. *Sustainable Cities and Society* 2017;35:764–73. doi:10.1016/j.scs.2017.09.032.
- [61] Korkas CD, Baldi S, Michailidis I, Kosmatopoulos EB. Occupancy-based demand response and thermal comfort optimization in microgrids with renewable energy sources and energy storage. *Applied Energy* 2016;163:93–104. doi:10.1016/j.apenergy.2015.10.140.
- [62] Yang R, Wang L. Multi-objective optimization for decision-making of energy and comfort management in building automation and control. *Sustainable Cities and Society* 2012;2:1–7. doi:10.1016/j.scs.2011.09.001.
- [63] A multi-stage optimization of pedestrian level wind environment and thermal comfort with lift-up design in ideal urban canyons. *Sustainable Cities and Society* 2019;46:101424. doi:10.1016/j.scs.2019.101424.
- [64] Carlucci S, Causone F, De Rosa F, Pagliano L. A review of indices for assessing visual comfort with a view to their use in optimization processes to support building integrated design. *Renewable and Sustainable Energy Reviews* 2015;47:1016–33. doi:10.1016/j.rser.2015.03.062.
- [65] Vera S, Uribe D, Bustamante W, Molina G. Optimization of a fixed exterior complex fenestration system considering visual comfort and energy performance criteria. *Building and Environment* 2017;113:163–74. doi:10.1016/j.buildenv.2016.07.027.
- [66] Yu T-H, Kwon S-Y, Im K-M, Lim J-H. An RTP-based dimming control system for visual comfort enhancement and energy optimization. *Energy and Buildings* 2017;144:433–44. doi:10.1016/j.enbuild.2016.04.045.
- [67] Tunzi M, Boukhanouf R, Li H, Svendsen S, Ianakiev A. Improving thermal performance of an existing UK district heat network: A case for temperature optimization. *Energy and Buildings* 2018;158:1576–85. doi:10.1016/j.enbuild.2017.11.049.
- [68] Chen X, Yang H. A multi-stage optimization of passively designed high-rise residential buildings in multiple building operation scenarios. *Applied Energy* 2017;206:541–57. doi:10.1016/j.apenergy.2017.08.204.
- [69] Tronchin L, Manfren M, Tagliabue LC. Optimization of building energy performance by means of multi-scale analysis – Lessons learned from case studies. *Sustainable Cities and Society* 2016;27:296–306. doi:10.1016/j.scs.2015.11.003.
- [70] Landsman J, Brager G, Doctor-Pingel M. Performance, prediction, optimization, and user behavior of night ventilation. *Energy and Buildings* 2018;166:60–72. doi:10.1016/j.enbuild.2018.01.026.
- [71] Carreira P, Costa AA, Mansur V, Arsénio A. Can HVAC really learn from users? A simulation-based study on the effectiveness of voting for comfort and energy use optimization. *Sustainable Cities and Society* 2018;41:275–85. doi:10.1016/j.scs.2018.05.043.
- [72] Ascione F, Bianco N, De Stasio C, Mauro GM, Vanoli GP. A new comprehensive approach for cost-optimal building design integrated with the multi-objective model predictive control of HVAC systems. *Sustainable Cities and Society* 2017;31:136–50. doi:10.1016/j.scs.2017.02.010.
- [73] Zhang A, Bokel R, van den Dobbela A, Sun Y, Huang Q, Zhang Q. Optimization of thermal and daylight performance of school buildings based on a multi-objective genetic algorithm in the cold climate of China. *Energy and Buildings* 2017;139:371–84. doi:10.1016/j.enbuild.2017.01.048.

- [74] Negendahl K, Nielsen TR. Building energy optimization in the early design stages: A simplified method. *Energy and Buildings* 2015;105:88–99. doi:10.1016/j.enbuild.2015.06.087.
- [75] Yu W, Li B, Jia H, Zhang M, Wang D. Application of multi-objective genetic algorithm to optimize energy efficiency and thermal comfort in building design. *Energy and Buildings* 2015;88:135–43. doi:10.1016/j.enbuild.2014.11.063.
- [76] Wright JA, Brownlee A, Mourshed MM, Wang M. Multi-objective optimization of cellular fenestration by an evolutionary algorithm. *Journal of Building Performance Simulation* 2014;7:33–51. doi:10.1080/19401493.2012.762808.
- [77] Shi X, Tian Z, Chen W, Si B, Jin X. A review on building energy efficient design optimization from the perspective of architects. *Renewable and Sustainable Energy Reviews* 2016;65:872–84. doi:10.1016/j.rser.2016.07.050.
- [78] Yang R, Wang L. Multi-zone building energy management using intelligent control and optimization. *Sustainable Cities and Society* 2013;6:16–21. doi:10.1016/j.scs.2012.07.001.
- [79] Esmaeilzadeh A, Zakerzadeh MR, Koma AY. The comparison of some advanced control methods for energy optimization and comfort management in buildings. *Sustainable Cities and Society* 2018;43:601–23. doi:10.1016/j.scs.2018.08.038.
- [80] Roshan G, Rousta I, Ramesh M. Studying the Effects of Urban Sprawl of Metropolis on Tourism - Climate Index Oscillation: A Case Study of Tehran City. vol. 2. 2010. doi:10.5897/JGRP09.069.
- [81] Bashiri A, Alizadeh SH. The analysis of demographics, environmental and knowledge factors affecting prospective residential PV system adoption: A study in Tehran. *Renewable and Sustainable Energy Reviews* 2018;81:3131–9. doi:10.1016/j.rser.2017.08.093.
- [82] Jia J, Lee WL. The rising energy efficiency of office buildings in Hong Kong. *Energy and Buildings* 2018;166:296–304. doi:10.1016/j.enbuild.2018.01.062.
- [83] Machairas V, Tsangrassoulis A, Axarli K. Algorithms for optimization of building design: A review. *Renewable and Sustainable Energy Reviews* 2014;31:101–12. doi:10.1016/j.rser.2013.11.036.
- [84] Hamdy M, Nguyen A-T, Hensen JLM. A performance comparison of multi-objective optimization algorithms for solving nearly-zero-energy-building design problems. *Energy and Buildings* 2016;121:57–71. doi:10.1016/j.enbuild.2016.03.035.
- [85] Tuhus-Dubrow D, Krarti M. Genetic-algorithm based approach to optimize building envelope design for residential buildings. *Building and Environment* 2010;45:1574–81. doi:10.1016/j.buildenv.2010.01.005.
- [86] Bornatico R, Pfeiffer M, Witzig A, Guzzella L. Optimal sizing of a solar thermal building installation using particle swarm optimization. *Energy* 2012;41:31–7. doi:10.1016/j.energy.2011.05.026.
- [87] Chiandussi G, Codegone M, Ferrero S, Varesio FE. Comparison of multi-objective optimization methodologies for engineering applications. *Computers & Mathematics with Applications* 2012;63:912–42. doi:10.1016/j.camwa.2011.11.057.
- [88] Negendahl K. Building performance simulation in the early design stage: An introduction to integrated dynamic models. *Automation in Construction* 2015;54:39–53. doi:10.1016/j.autcon.2015.03.002.
- [89] Yigit S, Ozorhon B. A simulation-based optimization method for designing energy efficient buildings. *Energy and Buildings* 2018;178:216–27. doi:10.1016/j.enbuild.2018.08.045.

- [90] Agirbas A. Façade form-finding with swarm intelligence. *Automation in Construction* 2019;99:140–51. doi:10.1016/j.autcon.2018.12.003.
- [91] Konis K, Gamas A, Kensek K. Passive performance and building form: An optimization framework for early-stage design support. *Solar Energy* 2016;125:161–79. doi:10.1016/j.solener.2015.12.020.
- [92] Zhang L, Zhang L, Wang Y. Shape optimization of free-form buildings based on solar radiation gain and space efficiency using a multi-objective genetic algorithm in the severe cold zones of China. *Solar Energy* 2016;132:38–50. doi:10.1016/j.solener.2016.02.053.
- [93] Yi YK, Malkawi AM. Optimizing building form for energy performance based on hierarchical geometry relation. *Automation in Construction* 2009;18:825–33. doi:10.1016/j.autcon.2009.03.006.
- [94] Kämpf JH, Montavon M, Bunyesc J, Bolliger R, Robinson D. Optimisation of buildings' solar irradiation availability. *Solar Energy* 2010;84:596–603. doi:10.1016/j.solener.2009.07.013.
- [95] Huang Y-S, Chang W-S, Shih S-G. Building Massing Optimization in the Conceptual Design Phase. *Computer-Aided Design and Applications* 2015;12:344–54. doi:10.1080/16864360.2014.981465.
- [96] Jin J-T, Jeong J-W. Thermal characteristic prediction models for a free-form building in various climate zones. *Energy* 2013;50:468–76. doi:10.1016/j.energy.2012.11.011.
- [97] Jalaei F, Jrade A. Integrating building information modeling (BIM) and LEED system at the conceptual design stage of sustainable buildings. *Sustainable Cities and Society* 2015;18:95–107. doi:10.1016/j.scs.2015.06.007.
- [98] Javanroodi K, Mahdavinejad M, Nik VM. Impacts of urban morphology on reducing cooling load and increasing ventilation potential in hot-arid climate. *Applied Energy* 2018;231:714–46. doi:10.1016/j.apenergy.2018.09.116.
- [99] Zinzi M, Carnielo E, Mattoni B. On the relation between urban climate and energy performance of buildings. A three-years experience in Rome, Italy. *Applied Energy* 2018;221:148–60. doi:10.1016/j.apenergy.2018.03.192.
- [100] Allegrini J, Dorer V, Carmeliet J. Coupled CFD, radiation and building energy model for studying heat fluxes in an urban environment with generic building configurations. *Sustainable Cities and Society* 2015;19:385–94. doi:10.1016/j.scs.2015.07.009.
- [101] Emadodin I, Taravat A, Rajaei M. Effects of urban sprawl on local climate: A case study, north central Iran. *Urban Climate* 2016;17:230–47. doi:10.1016/j.uclim.2016.08.008.
- [102] Peel MC, Finlayson BL, McMahon TA. Updated world map of the Köppen-Geiger climate classification. *Hydrol Earth Syst Sci* 2007;11:1633–44. doi:10.5194/hess-11-1633-2007.
- [103] I.R. of Iran Meteorological Organizaiton (IRIMO) n.d. <http://reports.irimo.ir/jasperserver/login.html> (accessed May 25, 2018).
- [104] Executive code of building Conservation from Fire, Code 112. Tehran: State Management and Planning Organization; 1992.
- [105] Terms and conditions of zoning in Tehran. Tehran: Tehran Urban Research and Planing center; 2010.
- [106] Design Criteria and locating of high-rise buildings in Tehran. Tehran: Zista Consultant and Tadbir Baft Consultant; 1998.
- [107] Watson R, Chapman K. Radiant Heating and Cooling Handbook | Hvac | Heat Transfer. 1st ed. NewYork: McGraw-Hill Professional; 2002.

- [108] Heidari S, Sharples S. A comparative analysis of short-term and long-term thermal comfort surveys in Iran. *Energy and Buildings* 2002;34:607–14. doi:10.1016/S0378-7788(02)00011-7.
- [109] McIntyre DA. Chamber studies—reductio ad absurdum? *Energy and Buildings* 1982;5:89–96. doi:10.1016/0378-7788(82)90003-2.
- [110] Heidari S. Comfort Temperature of Iranian People in City of Tehran. *Honarhayeh_Ziba* 2009;1:5–14.

ACCEPTED MANUSCRIPT